Journal of Sound and Vibration 333 (2014) 5657–5679

Contents lists available at ScienceDirect

Journal of Sound and Vibration

journal homepage: www.elsevier.com/locate/jsvi

Semi-active friction tendons for vibration control of space structures

Hernán Garrido, Oscar Curadelli *, Daniel Ambrosini

Engineering Faculty, National University of Cuyo, CONICET, Parque Gral. San Martín, Mendoza, Argentina

ARTICLE INFO

Article history:
Received 23 May 2013
Received in revised form
21 May 2014
Accepted 12 June 2014
Handling Editor: D.J. Wagg
Available online 8 July 2014

ABSTRACT

Semi-active vibration control systems are becoming popular because they offer both the reliability of passive systems and the versatility of active control without high power demands. In this work, a new semi-active control system is proposed and studied numerically. The system consists of variable-friction dampers linked to the structure through cables. Auxiliary soft springs in parallel with these friction dampers allow them to return to their initial pre-tensioned state. Using cables makes the system suitable for deployable, flexible and lightweight structures, such as space structures (spacecraft). A control system with three control laws applied to a single-degree-of-freedom structure is studied. Two of these laws are derived by using Lyapunov theory, whereas the third one is developed heuristically. In order to assess the performance of the control system, a parametric study is carried out through numerical simulations. An application of the proposed method to multi-degree-of-freedom structures is also presented and demonstrated through a numerical example. The system in semi-active mode is more effective than in passive mode and its effectiveness is less sensitive to loss of pre-tension.

1. Introduction

The use of passive systems is the simplest and most reliable approach for vibration control. Passive vibration control can be classified into: (1) structural damping (e.g. [1,2]), (2) supplemental passive damping [3], and (3) passive isolation [4]. Notwithstanding their advantages, in some cases the performance of passive systems is not good enough, or it is necessary heavy equipment to reach the desired performance. Moreover, passive systems are not automatically adaptive to changes in the properties of the controlled structure or in the magnitude and frequency content of the excitation.

On the other hand, active vibration control is very attractive and powerful. Although many works have been published on the subject (e.g. [5,6]), the technology has some inherent problems: instability due spillover [7] and high power demands. The latter is a limitation in some special applications such as the vibration mitigation in space structures.

An attractive alternative is semi-active vibration control. The semi-active approach consists in smartly modifying characteristics (e.g. inertia, stiffness, or more commonly damping) of special devices coupled to the structure that is to be controlled. In general, semi-active systems are stable, adaptive, relatively good performing, and low-power consuming [7]. In some cases, it is even possible to harvest the vibrational energy of the disturbed structure [8].

* Corresponding author. Tel.: +54 261 4135000x2195.
E-mail addresses: carloshernangarrido@yahoo.com.ar (H. Garrido), ocuradelli@fing.uncu.edu.ar (O. Curadelli).

http://dx.doi.org/10.1016/j.jsv.2014.06.018
0022-460X/

The main goal of the present research is to propose and numerically study a novel semi-active vibration control system suitable for space structures. Such structures, namely the large space structures, have the flowing characteristics [9]:

1. in general, they consist of a central rigid body with large flexible appendages;
2. their natural damping is very poorly known and very light ($\sim$ 0.5 percent critical);
3. prediction of their behavior in space via on-earth testing is quite limited;
4. vibration suppression criteria are very stringent.

Since in space applications volume and weight of any accessory system (such as the vibration control system) is prohibitive, every space structures are lightweight and many of them are deployable [10].

A typical problem in vibration control is the design of the bracing system which couples the dampers to the structure. Usually, bracing systems which are designed to resist compression without buckling are heavy and voluminous, and therefore inappropriate for space structures. In order to deal with the buckling problem, Golafshani et al. [11] proposed a friction semi-active device with permanent presence of stiffness, also capable of absorbing the input energy using the maximum capacity of the brace. Rahani et al. [12] investigated the same concept, but considering the use of a variable viscous damper. Among the many types of structural elements, cables distinguish themselves in that they can be packaged in a compact volume and yet retain the same structural properties as rod elements when extended [13]. This fact suggests that cables could be very advantageous as bracing system in vibration control of space structures.

Taut-cable theory [14] has been traditionally employed for simulating the dynamics of cable networks. However, the phenomenon of cable slackening deserves special attention in the proposed vibration control system. Cable slackening has been studied in different contexts. For example, Guevara and McClure [15] studied the nonlinear seismic response of an antenna-supporting structure in which the stress–strain law of cables is defined only in tension. Mitsugi [13] presented a nonlinear static analysis method for cable networks in which cables under compressive strain are canceled. Casciati and Ubertini [16], in their work on nonlinear vibration of shallow cables with semi-active Tuned Mass Damper (TMD), studied the effect of detuning due to cable slackening. Recent works which include the slackening phenomenon in their models are [17–19].

None of those works proposes methods to prevent the cables from slackening explicitly, apart from initial pre-tension. Recently, Wang et al. [20] proposed an active shape adjustment in which the slackening is explicitly addressed by means of PZT actuators placed in series with some structural cables to modify their tension; similar to the approach used by Preumont [21], Smrz et al. [22], and Guo et al. [23] to add active damping to a cable structure.

In this work, it is proposed a new vibration control system, called Semi-active Friction Tendons, which has the following characteristics:

1. it is a semi-active system, which is adaptive, relatively effective, and low power consuming;
2. it is based on dry friction dampers using piezoelectric stack actuators to apply the normal forces (i.e. piezoelectric friction dampers), thus it is suitable in space environment (vacuum);
3. each friction damper is coupled to the structure through a cable, therefore the control system is very lightweight and also compatible with the concept of deployable structure;
4. the probable slackening of cables, due to a cable cannot exert compressive force to its friction damper, is mitigated by means of: (1) an auxiliary soft spring in parallel with each friction damper (giving a small pre-tension to the corresponding cable, as in [24]), and (2) an appropriate semi-active control strategy;
5. the pre-tension force is be very small and (when possible) the tendons can be placed as symmetric pairs, thus the equilibrium point of the structure does not change after the installation of the control system.

A detailed study on the performance of Semi-active Friction Tendons is carried out in an idealized single-degree-of-freedom (SDOF) structural model. Then, the control system is applied to a multi-degree-of-freedom (MDOF) structure.

2. Description of the control system

It is proposed a device consisting of a dry-friction damper in parallel with an auxiliary soft spring, in which one end is fixed to the reference frame, and the other end is in series with a cable which links the friction damper to the structure that is to be controlled. This device is named Semi-active Friction Tendon, and it is shown in Fig. 1a.

The friction damper consists of three friction pads, two of them are fixed and the third one is mobile; see Fig. 1b. To induce friction at the interfaces between the pads, normal forces are applied by a piezoelectric stack actuator which allows the use of advanced control strategies [25]. This type of actuator is used because of its large bandwidth, and large forces that can be generated with low power consuming (as compared to the structural energy which can be dissipated through friction).

In order to gain insight into the intrinsic characteristics of the proposed control system, a pair of semi-active friction tendons on a SDOF oscillator is considered. Such configuration is shown in Fig. 2.

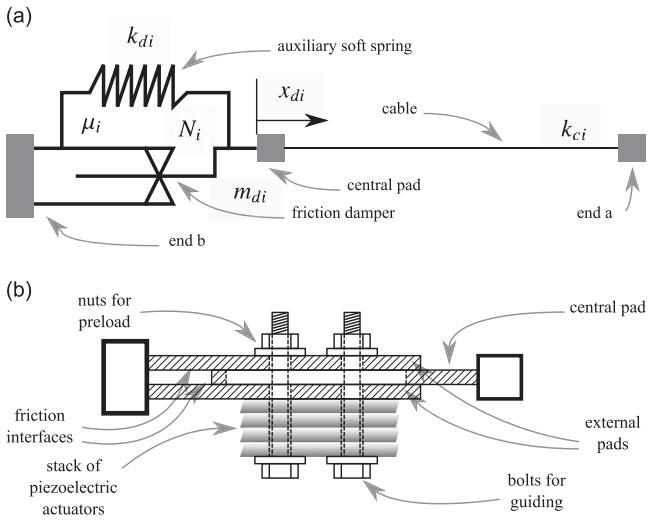

Fig. 1. Schematic representation of the proposed device: (a) semi-active friction tendon; (b) detail of the friction damper.

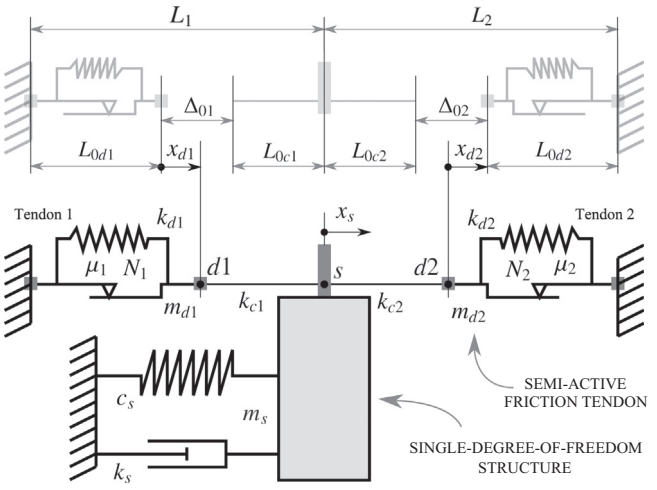

Fig. 2. SDOF structure controlled by two semi-active friction tendons. Reference: Grey lines match to natural shapes, and black lines to equilibrium- and tensioned-state shapes.

3. Nonlinear model

3.1. Modeling preliminaries

3.1.1. Cables

The pre-tensions of the tendons are defined, in terms of length stretching, as follows:

$$\Delta_{0i} = L_i - L_{0ci} - L_{0di} \quad \text{for } i = 1, 2, \tag{1}$$

in which L_i is the final length in static- and tensioned-state of tendon i; L_{0ci} and L_{0di} are, respectively, the natural (i.e. un-tensioned) lengths of the cable and the spring of tendon i; see Fig. 2. Note that relaxation or yielding of the cable causes a reduction in pre-tension Δ_{0i} due to the increment in L_{0ci}.

In this work, cables are assumed to act only in tension with constant stiffness, and their tension forces are given by

$$F_{c1} = k_{c1}\ \text{sat}(x_s - x_{d1} + \Delta_{01}), \tag{2}$$

$$F_{c2} = k_{c2}\ \text{sat}(-x_s + x_{d2} + \Delta_{02}), \tag{3}$$

in which k_{ci} and x_{di} are, respectively, the tension stiffnesses and the deformation of the auxiliary soft spring of the tendon i (for sign convention, see Fig. 2); x_s is the displacement of the structure respect of its original position, and sat is a saturation

function defined as

$$\mathrm{sat}(x)=\begin{cases}0 & \text{if } x\in(-\infty,0]\\ x & \text{if } x\in(0,\infty).\end{cases} \tag{4}$$

3.1.2. Friction dampers

During relative motion, a normal force is applied by piezoelectric actuators to induce friction force at the contact interface between the moving and fixed friction pads. Each actuator consists of a number of piezoelectric layers in a stack. After taking some constitutive and constructive considerations, the normal force can be stated as [26]

$$N=N_0+\Delta N u, \tag{5}$$

in which N_0 is a pre-load force applied to ensure the contact between the surfaces of the pads; ΔN is a modulation term which depends on the piezoelectric stack actuator characteristics, the maximal voltage applied, and the stiffness of the device itself; and u is a dimensionless command signal (the pre-load value N_0 and the range of variation of u must ensure the condition $N\geq 0$).

In view of that, in this work it is considered that the normal force of each friction damper can be instantaneously adjusted in the following range:

$$N_{i\min}<N_i<N_{i\max} \quad \text{for } i=1,2, \tag{6}$$

with $N_{i\min}\geq 0$, for $i=1,2$.

Assuming steady-state motion, with operating conditions such that the velocity of the mobile pad is much higher than the Stribeck velocity, and if the viscous damping is neglected with respect to the friction damping, then the friction force of each friction damper can be expressed as [25]

$$F_{fi}=\mu_i N_i\ \mathrm{sgn}(\dot{x}_{di}) \quad \text{for } i=1,2, \tag{7}$$

which match with the classical Coulomb's friction law, being $\mu_i=2\mu_{mi}$, where μ_{mi} is the dynamic friction coefficient of the materials used in the friction damper i; and $\dot{x}_{di}$ the velocity of the mobile pad i. Note that, according to the work of Dupont [27], more sophisticated friction models would conduce to Lyapunov-based control strategies similar to those developed from classical Coulomb's model.

3.2. Equations of motion

Considering the expressions (2), (3), (7), and Fig. 2, the equations of motion of the system can be expressed as

$$m_s\ddot{x}_s+c_s\dot{x}_s+k_s x_s+F_{c1}-F_{c2}=f_{es}, \tag{8}$$

$$m_{d1}\ddot{x}_{d1}+k_{d1}x_{d1}+F_{f1}-F_{c1}=f_{ed1}, \tag{9}$$

$$m_{d2}\ddot{x}_{d2}+k_{d2}x_{d2}+F_{f2}+F_{c2}=f_{ed2}, \tag{10}$$

where m_s, c_s and k_s are the mass, the damping coefficient, and the stiffness of the structure to be controlled; $m_{d\,1}$ and $m_{d\,2}$ are the masses of the mobile pads; $k_{d\,1}$ and $k_{d\,2}$ are the stiffnesses of the auxiliary soft springs; and f_{es}, $f_{ed\,1}$ and $f_{ed\,2}$ are external forces applied to the mass of the structure, and to the masses of mobile pads 1 and 2, respectively.

3.3. State-space representation

In order to simplify the design of feedback laws with the Lyapunov direct method, the nonlinear system can be written in state-space form given as

$$\dot{\mathbf{x}}=\mathbf{f}(\mathbf{x})+\mathbf{u}_e, \tag{11}$$

$\mathbf{x}$ being the state vector, defined as

$$\mathbf{x}=[x_s\ \ x_{d1}\ \ x_{d2}\ \ \dot{x}_s\ \ \dot{x}_{d1}\ \ \dot{x}_{d2}]^T; \tag{12}$$

$\mathbf{u}_e$ the vector of external excitations; $\mathbf{f}\colon \mathbb{R}^6\to\mathbb{R}^6$ the following smooth vector function:

$$\mathbf{f}(\mathbf{x})=\begin{bmatrix}\dot{x}_s\\ \dot{x}_{d1}\\ \dot{x}_{d2}\\ \frac{1}{m_s}\left(-k_s x_s-c_s\dot{x}_s-k_{c1}\ \mathrm{sat}(x_s-x_{d1}+\Delta_{01})+k_{c2}\ \mathrm{sat}(-x_s+x_{d2}+\Delta_{02})\right)\\ \frac{1}{m_{d1}}\left(-k_{d1}x_{d1}-\mu_1 N_1\ \mathrm{sgn}(\dot{x}_{d1})+k_{c1}\ \mathrm{sat}(x_s-x_{d1}+\Delta_{01})\right)\\ \frac{1}{m_{d2}}\left(-k_{d2}x_{d2}-\mu_2 N_2\ \mathrm{sgn}(\dot{x}_{d2})-k_{c2}\ \mathrm{sat}(-x_s+x_{d2}+\Delta_{02})\right)\end{bmatrix}; \tag{13}$$

and $\mathbf{u}_e$ the vector of external excitations, defined as

$$\mathbf{u}_e = \left[0 \;\; 0 \;\; 0 \;\; \frac{f_{es}}{m_s} \;\; \frac{f_{ed1}}{m_{d1}} \;\; \frac{f_{ed2}}{m_{d2}}\right]^T. \tag{14}$$

To ensure geometric and stiffness symmetry (relative to the mass of the oscillator), it is assumed that

$$k_{d1} = k_{d2} = k_d, \quad m_{d1} = m_{d2} = m_d, \quad k_{c1} = k_{c2} = k_c, \quad \Delta_{01} = \Delta_{02} = \Delta_0, \quad L_{0d1} = L_{0d2}, \quad L_{0c1} = L_{0c2}, \quad \mu_1 = \mu_2 = \mu. \tag{15}$$

Then, the nonlinear system (11) has one equilibrium point at

$$\mathbf{x}_0 = [0 \;\; x_{d10} \;\; x_{d20} \;\; 0 \;\; 0 \;\; 0]^T, \tag{16}$$

where $x_{d10} = -x_{d20}$, being $x_{d10} > 0$. For details, see Appendix A.

4. Semi-active control laws

In order to control the semi-active devices, three control laws are developed. The first control law is developed from Lyapunov's stability-theory, yielding a *quickest-descent controller* which has already been studied in the literature [28]. The second control law introduces some assumptions on the former one, which are applicable due to the mechanical configuration of the considered system, resulting in a novel control law with interesting features. The third control law is developed from a heuristic approach aiming to prevent the cable from slackening.

4.1. Direct-Lyapunov control laws

Since the objective of vibration control is to mitigate the vibration energy of the structure, it is considered only the structural subsystem, i.e.,

$$\begin{bmatrix} \dot{x}_s \\ \ddot{x}_s \end{bmatrix} = \begin{bmatrix} \dot{x}_s \\ \frac{1}{m_s}(-k_s x_s - c_s \dot{x}_s - F_{c1} + F_{c2}) \end{bmatrix} + \begin{bmatrix} 0 \\ \frac{f_{es}}{m_s} \end{bmatrix}. \tag{17}$$

In the design of the control laws, the forces exerted by the cables are the controllable inputs.

The subsystem (17) has an equilibrium point at $[x_s \;\; \dot{x}_s]^T = [0 \;\; 0]^T$ (see Appendix A), and therefore the direct method of Lyapunov can be applied.

Introduce the following function:

$$V(\mathbf{z}) = \mathbf{z}^T \mathbf{P} \mathbf{z}, \tag{18}$$

in which $\mathbf{z} = [x_s \;\; \dot{x}_s]^T$ is the state vector of the subsystem (17); and $\mathbf{P}$ is a real, symmetric, and positive definite matrix, in such a way that $V(\mathbf{z})$ is a valid Lyapunov function candidate. In this research $V(\mathbf{z})$ is considered to be equal to the vibration energy of the structure (plus the elastic energy in the auxiliary soft springs), then $\mathbf{P}$ is defined as

$$\mathbf{P} = \frac{1}{2}\begin{bmatrix} k_s + 2k_d & 0 \\ 0 & m_s \end{bmatrix}. \tag{19}$$

The rate of change of energy in the subsystem (17) is [28]

$$\dot{V}(\mathbf{z}) = \mathbf{z}^T \mathbf{P} \dot{\mathbf{z}} + \dot{\mathbf{z}}^T \mathbf{P} \mathbf{z}. \tag{20}$$

Substituting expressions (17) and (19) in (20), the following derivative of the Lyapunov function candidate is obtained:

$$\dot{V}(\mathbf{z}) = m_s \dot{x}_s \ddot{x}_s + (k_s + 2k_d) x_s \dot{x}_s = \dot{x}_s(-c_s \dot{x}_s - k_s x_s - F_{c1} + F_{c2} + f_{es}) + (k_s + 2k_d) x_s \dot{x}_s, \tag{21}$$

which, after cancelation conduces to

$$\dot{V}(\mathbf{z}) = -c_s \dot{x}_s^2 + \dot{x}_s(F_{c2} - F_{c1}) + \dot{x}_s f_{es} + 2k_d x_s \dot{x}_s. \tag{22}$$

The goal of this type of control is to make $\dot{V}(\mathbf{z})$ as low as possible. Hence, this kind of control algorithms are often referred to in the literature as *quickest-descent controllers* [28].

4.1.1. Quickest-descent control law

From the equations of motion (9) and (10), considering conditions (15), the cable forces can be rewritten as

$$F_{c1} = m_d \ddot{x}_{d1} + k_d x_{d1} + F_{f1} - f_{ed1}, \tag{23}$$

$$F_{c2} = -m_d \ddot{x}_{d2} - k_d x_{d2} - F_{f2} + f_{ed2}, \tag{24}$$

where $F_{f\,1}$ and $F_{f\,2}$ are the controllable terms.

Replacing Eqs. (23) and (24) in expression (22) results in

$$\dot{V}(\mathbf{z}) = \dot{x}_s(f_{es} + f_{ed1} + f_{ed2}) + 2k_d x_s \dot{x}_s - c_s \dot{x}_s^2 - \dot{x}_s(m_d \ddot{x}_{d1} + k_d x_{d1} + F_{f1} + m_d \ddot{x}_{d2} + k_d x_{d2} + F_{f2}), \tag{25}$$

which, using (7), becomes

$$\dot{V}(\mathbf{z}) = \dot{x}_s(f_{es}+f_{ed1}+f_{ed2})+2k_d x_s\dot{x}_s - c_s\dot{x}_s^2 - \dot{x}_s(m_d\ddot{x}_{d1}+k_d x_{d1}+m_d\ddot{x}_{d2}+k_d x_{d2}) - \dot{x}_s\mu N_1\,\mathrm{sgn}(\dot{x}_{d1}) - \dot{x}_s\mu N_2\,\mathrm{sgn}(\dot{x}_{d2}). \tag{26}$$

On the right-hand side of Eq. (26), the last two terms are the only ones that can be controlled by means of the actuators. The control objective is to make such terms as negative as possible. Applying the control constraints (6) to Eq. (26), noting that μ is non-negative, yields the *quickest-descent control law*, which is stated as follows:

$$N_i = \begin{cases} N_{i\min} & \text{if } \dot{x}_s\,\mathrm{sgn}(\dot{x}_{di}) \le 0 \\ N_{i\max} & \text{if } \dot{x}_s\,\mathrm{sgn}(\dot{x}_{di}) > 0 \end{cases} \quad \text{for } i = 1,2. \tag{27}$$

The *quickest-descent control law*, expressed in Eq. (27), has the following drawbacks:

1. three velocity sensors are needed in order to sens $\dot{x}_s$, $\dot{x}_{d1}$ and $\dot{x}_{d2}$;
2. due to the dynamics of the tendons, the presence of $\dot{x}_{d1}$ and $\dot{x}_{d2}$ in the control logic generates undesirable fast commutations in the actuators.

In order to overcome these disadvantages, a new control law that eliminates the necessity of sensing the velocity of the moving pads is presented below.

4.1.2. Simplified quickest-descent control law

By inspecting expression (22), and recalling that $F_{c\,1}$ and $F_{c\,2}$ are not negative, it is only necessary to know the sign of $\dot{x}_s$ to decide when it is convenient to maximize or minimize those forces. Thus, if $\dot{x}_s$ is greater than zero, then $F_{c\,1}$ must be maximized and $F_{c\,2}$ minimized. The opposite must be done if $\dot{x}_s$ is less than zero.

Introduce the following assumptions:

$$\text{if } \dot{x}_s > 0 \text{ then } \dot{x}_{d1} \ge 0, \tag{28}$$

$$\text{if } \dot{x}_s < 0 \text{ then } \dot{x}_{d2} \le 0, \tag{29}$$

which are supposed to be true most of the time. This is confirmed by simulations in Section 5.2.2.

From (7), (23) and (24), it can be said that:

1. assumption (28) implies that if $\dot{x}_s > 0$, then $F_{c\,1}$ can be increased by increasing N_1;
2. similarly, (29) implies that if $\dot{x}_s < 0$, then $F_{c\,2}$ can be increased by increasing N_2.

In view of this, the *simplified quickest-descent control law* is stated as follows:

$$N_1 = \begin{cases} N_{1\min} & \text{if } \dot{x}_s \le 0 \\ N_{1\max} & \text{if } \dot{x}_s > 0, \end{cases} \tag{30}$$

$$N_2 = \begin{cases} N_{2\min} & \text{if } \dot{x}_s \ge 0 \\ N_{2\max} & \text{if } \dot{x}_s < 0. \end{cases} \tag{31}$$

From expressions (30) and (31), it is evident that the switching frequency of the control signals (N_1 and N_2) is the same as that of the structure velocity, making this control law much less prone to chattering.

A Lyapunov-stability analysis of the proposed control system, along with useful design considerations, is provided in Appendix B.

4.2. Slackening-preventing control law

By pursuing to prevent the cable slackening and by using a heuristic approach, a new semi-active strategy is proposed in this subsection.

By sensing the forces $F_{c\,1}$ and $F_{c\,2}$ by means of load cells, it is possible to mitigate the slackening by decreasing the normal force of each friction damper when the corresponding cable is not under tension. This idea conduces to the following control logic:

$$N_i = \begin{cases} N_{i\min} & \text{if } F_{ci} = 0 \\ N_{i\max} & \text{if } F_{ci} > 0 \end{cases} \text{for } i = 1,2. \tag{32}$$

In order to smooth the chattering generated by the discontinuities in this control law (and by noise when measuring very small forces), a soft threshold ϵ_f near the switching point is proposed to replace the discontinuity [29]. Hence, the

Table 1
Simulation parameters.

$m_s = 17.55$ kg	$N_{1\max} = N_{2\max} = N_{\max} = 10$ N
$k_s = 3055$ N m^{-1}	$N_{1\min} = N_{2\min} = N_{\min} = 3$ N
$c_s = 9.262$ N s m^{-1} ($\zeta_s = 2\%$)	$\mu = 0.5$
$m_d = 0.5$ kg	$\Delta_0 = 0.010$ m
$k_d = 200$ N m^{-1}	$k_c = 8000$ N m^{-1}

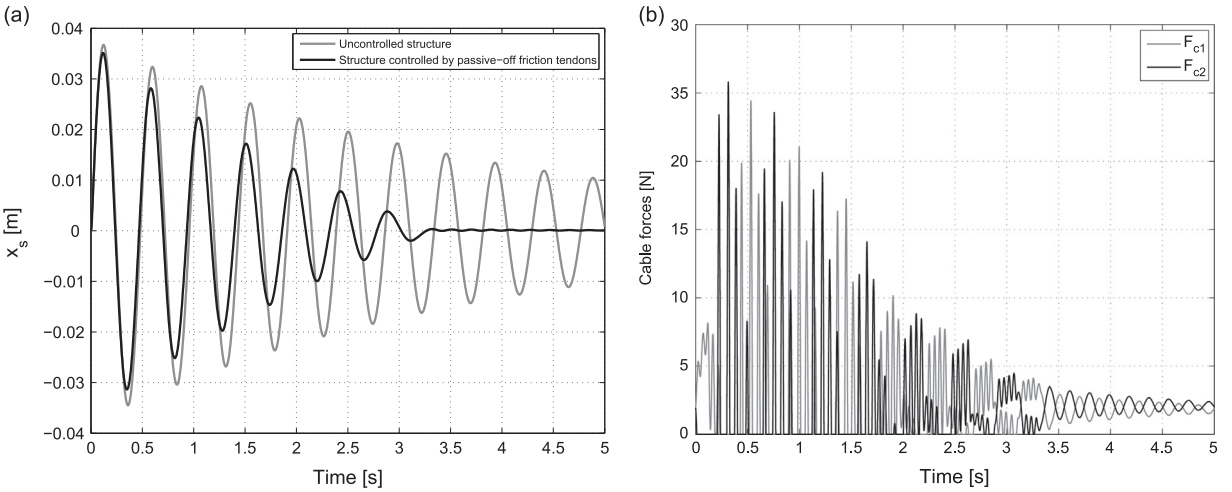

Fig. 3. Passive-off control mode: (a) absolute displacement response of the structure; (b) forces exerted by the cables.

slackening-preventing control law is stated as

$$N_i = \begin{cases} N_{i\min} + N_{\Delta i} F_{ci} & \text{if } F_{ci} \le \epsilon_f \\ N_{i\max} & \text{if } F_{ci} > \epsilon_f \end{cases} \quad \text{for } i = 1, 2, \tag{33}$$

in which $N_{\Delta i} = (N_{i\max} - N_{i\min})/\epsilon_f$ for $i = 1, 2$. This law enables to reduce the normal forces even though the cable forces are not exactly equal to zero.

The threshold ϵ_f must be large enough to prevent chattering problems; however, excessive values cause effectiveness reduction.

5. Simulations in a SDOF structural model

The simulation results given below demonstrate the effectiveness of the proposed control system in passive and semi-active modes applied on the structure of Fig. 2. The parameters of the simulated system (11) are given in Table 1, which correspond to future experimental studies, and the initial conditions are set at $\mathbf{x}_0$, given by (16). This simple model allows studying the main features and issues (e.g. effectiveness, cable slackening, and pre-tension effects) of the proposed vibration control system with passive- and semi-active-control in a clear and simple way.

In order to study the performance of the vibration control system, rigid body modes (if any) can be removed [21] and support acceleration (rigid body acceleration) $\ddot{x}_g$ can be considered as excitation in the simulations, i.e.,

$$f_{es} = -m_s \ddot{x}_g, \quad f_{ed1} = -m_{d1} \ddot{x}_g, \quad f_{ed2} = -m_{d2} \ddot{x}_g. \tag{34}$$

The signal $\ddot{x}_g$ is a rectangular pulse, with amplitude of -50 m s^{-2}, and duration of 0.01 s, which provides to the masses an initial velocity of 0.5 m s^{-1}. After the pulse ends, the system is under free oscillation conditions, allowing to characterize the properties of the control system.

As studied by Muanke et al. [25], friction-based vibration control systems have optimal values for the normal forces for a specified level of excitation. The design parameters $N_{\min}$ and $N_{\max}$ given in Table 1 have been selected below and above that optimal value.

5.1. Passive mode

In this case, the normal forces are considered to be held constant at minimal normal force $N_{\min}$ or at maximal normal force $N_{\max}$, hereinafter referred to as *passive-off mode* and *passive-on mode*, respectively. These cases, which are not optimal,

demonstrate the potential of semi-active control when applied to the proposed mechanical configuration. Optimum passive cases are addressed in Section 6.

5.1.1. Passive-off mode

Fig. 3a shows the response of the uncontrolled structure and the structure controlled with *passive-off mode*. The control system shows to be relatively effective in mitigating the oscillations of the structure.

From Fig. 3b, it is observed that the cables do not enter in a permanent slack-cable condition, which is due to

$$N_i < \frac{k_d \Delta_0}{\mu} \quad \text{for } i = 1,2 \tag{35}$$

(approximation assuming $k_d \ll k_c$). On the other hand, cable forces stabilize at a non-zero force which is equal to the initial pre-tension ($\approx k_d \Delta_0 = 2$ N). This fact is very important because allows the vibration control system to return to its initial conditions after the oscillation ends.

5.1.2. Passive-on mode

The response of the uncontrolled structure and the structure controlled with *passive-on mode* is shown in Fig. 4a.

By comparing Figs. 3a and 4a, it can be seen that, until 1.5 s, the system in *passive-on mode* displays smaller displacement than in *passive-off mode*, due to the larger control force exerted by the friction dampers through the cables (Figs. 3b and 4b). However, in the remaining time, the response is considerably larger in *passive-on mode* because a permanent slack-cable

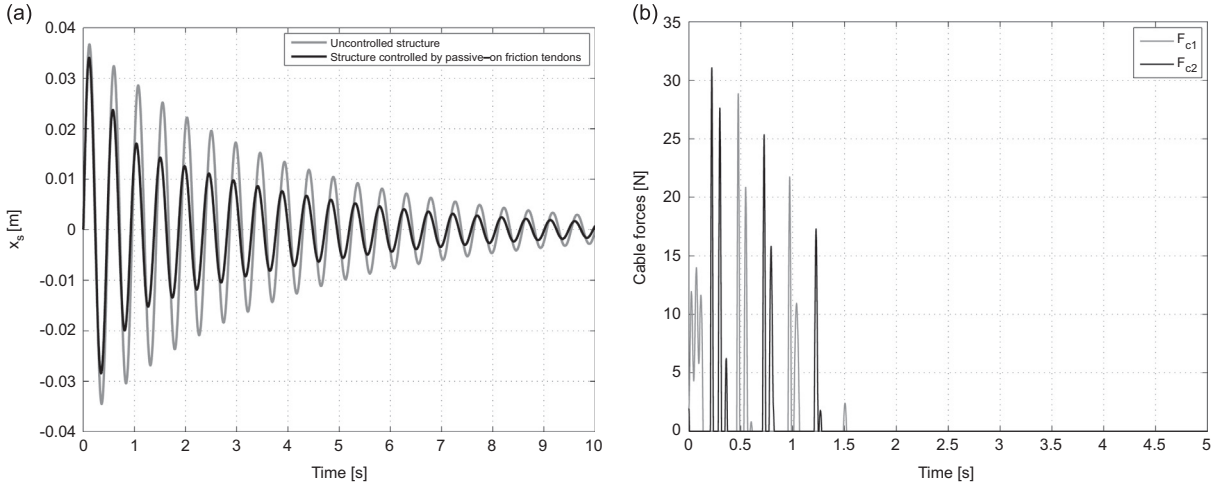

Fig. 4. Passive-on control mode: (a) absolute displacement response of the structure; (b) forces exerted by the cables.

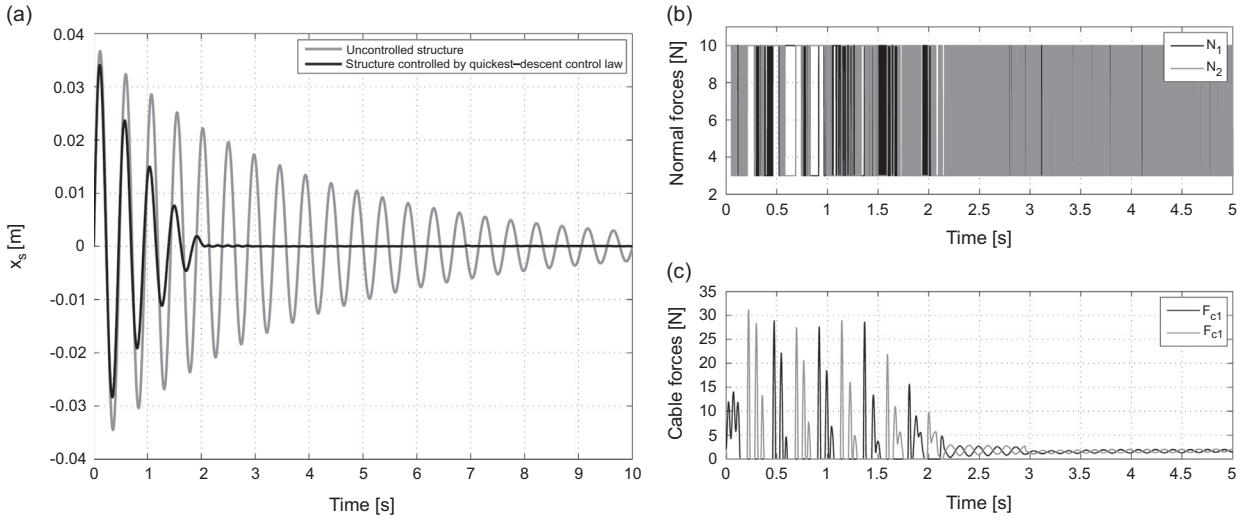

Fig. 5. Semi-active mode with *quickest-descent control law*: (a) absolute displacement response of the structure; (b) normal forces in the actuators; (c) forces exerted by the cables.

condition starts at 1.5 s disabling the control system. This can be seen in Fig. 4b as a stabilization of cable forces at zero force. Note that the permanent slack-cable condition makes the control system impractical under repetitive excitation.

5.2. Semi-active mode

Simulation results for the system (11) considering the normal forces are instantaneously adjusted according to the control laws developed in Section 4 are presented below.

5.2.1. Quickest-descent control law

Fig. 5a shows the displacements of the structure without control and controlled by using the *quickest-descent control law*. From Figs. 3a, 4a and 5a, it is clear that semi-active mode is more effective in reducing the displacement than both passive-off- and passive-on-modes.

As can be seen in Fig. 5c, the peaks of cable forces are as large as in *passive-on mode*. However, the cable forces stabilize at the initial pre-tension ($\approx k_d\Delta_0 = 2$ N) as in *passive-off mode* avoiding the permanent slack-cable condition, because

$$N_{i\min} < \frac{k_d\Delta_0}{\mu} \quad \text{for } i = 1,2 \tag{36}$$

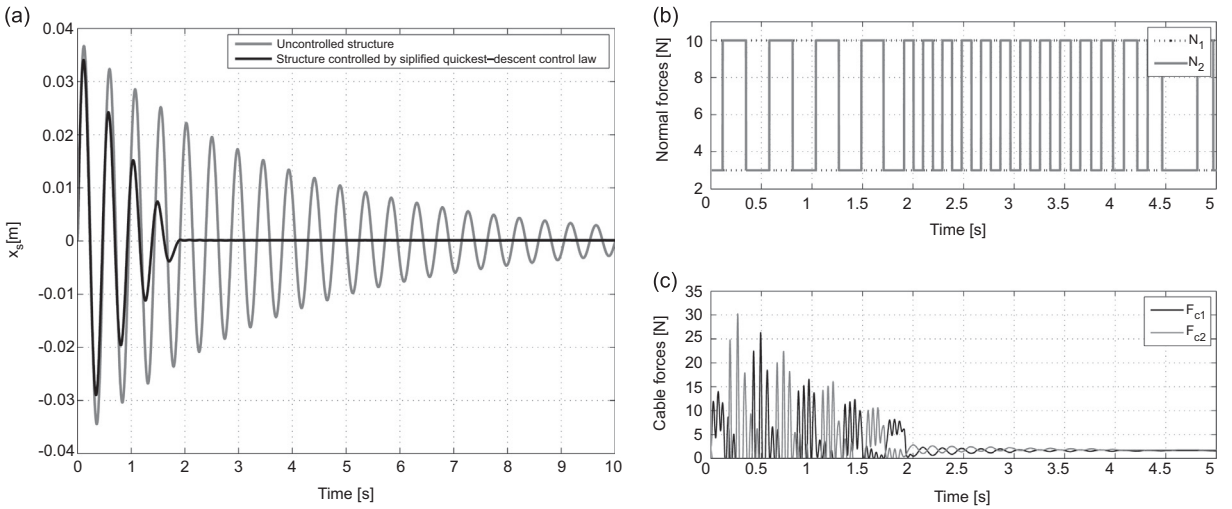

Fig. 6. Semi-active mode with *simplified quickest-descent control law*: (a) absolute displacement response of the structure; (b) normal forces in the actuators; (c) forces exerted by the cables.

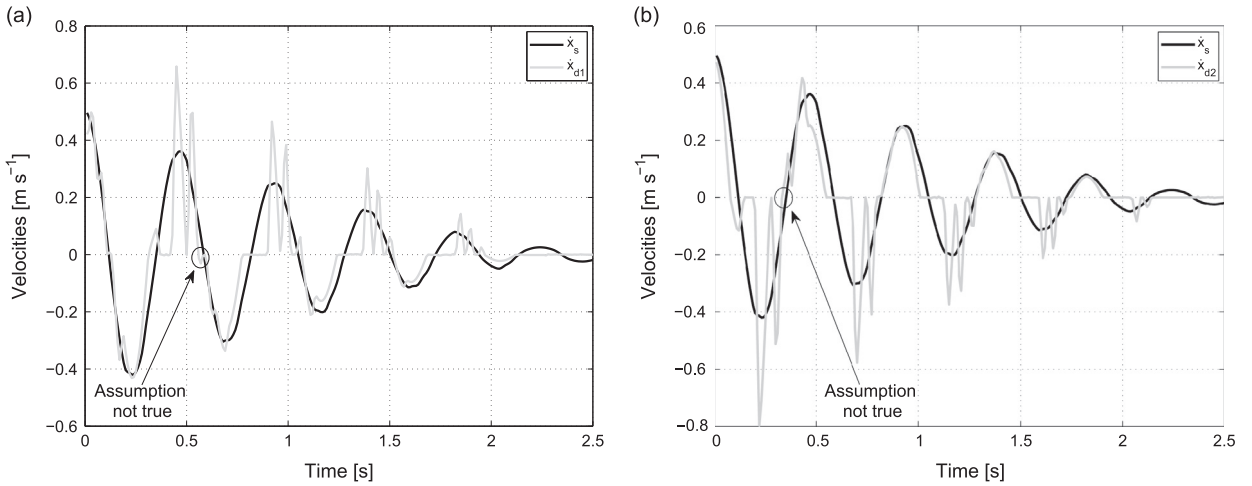

Fig. 7. Velocity of the structure compared with: (a) the velocity of the mobile pad of the friction damper 1; (b) the velocity of the mobile pad of the friction damper 2.

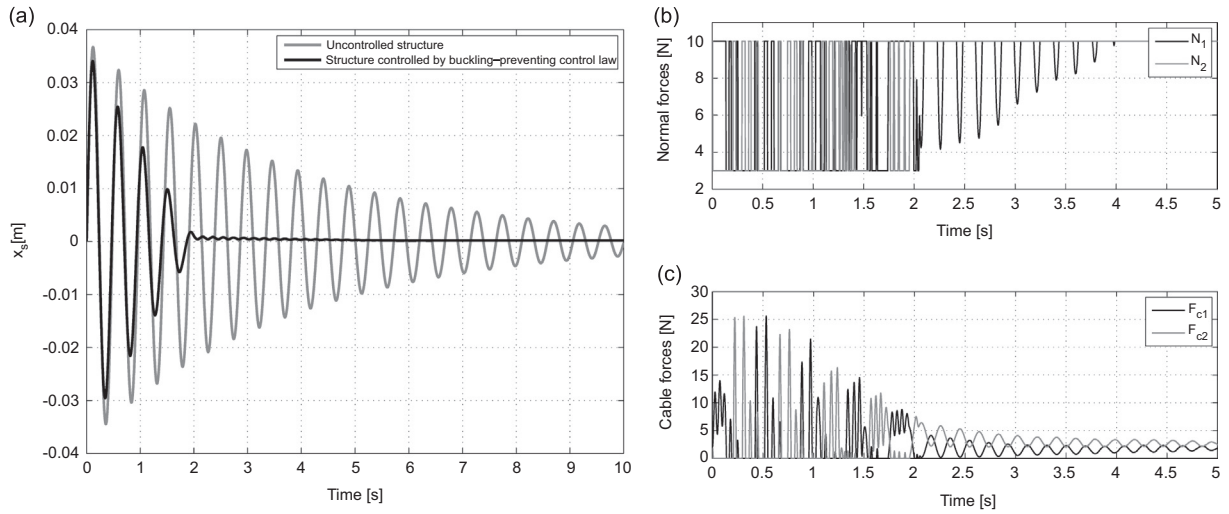

Fig. 8. Semi-active mode with *slackening-preventing control law*: (a) absolute displacement response of the structure; (b) normal forces in the actuators; (c) forces exerted by the cables.

(as in passive-off mode). The semi-active mode is more effective than both passive modes precisely because it combines the advantages of both of them.

The fast switching observed in Fig. 5b (chattering) can be reduced by using the *simplified quickest-descent control law* which is demonstrated below.

5.2.2. Simplified quickest-descent control law

Figs. 5a and 6a show that the effectiveness of the system using *quickest-descent control law* is very similar to that using *simplified quickest-descent control law*. However, with the former law, the forces exerted by the cables have slightly higher peaks (see Figs. 5c and 6c) and the switching frequency of the signals that command the actuators is much higher (see Figs. 5b and 6b).

In order to demonstrate the assumptions (28) and (29) stated in Section 4.1.2, in Fig. 7 it can be observed that the signs of the velocities of the structure ($\dot{x}_s$) and of the mobile pads ($\dot{x}_{d1}$ and $\dot{x}_{d2}$) are virtually coincident.

5.2.3. Slackening-preventing control law

Simulations of the system in semi-active mode using *slackening-preventing control law*, in which the normal forces are instantaneously adjusted according to (33), with ϵ_f=1 N, are presented in Fig. 8.

A comparison of Figs. 5a, 6a, and 8a shows that this control law has an effectiveness in the control of the displacement similar to the previous two control laws.

Fig. 8b shows that the switching frequency of the command signals is similar to that of the cable forces (lower than that of the *quickest-descent control law* but higher than that of the *simplified quickest-descent control law*). From Fig. 8c, it is observed that the slack-cable problem is avoided, since the cable forces stabilize at a non-zero force. Fig. 8b and c shows that from t=2 s, when the cable force of Tendon 1 remains above the threshold ϵ_f (t=4 s, for Tendon 2), the corresponding command signal stops switching.

6. Parametric study in a SDOF structural model

In order to demonstrate the combined effect of normal forces on the friction dampers, pre-tension of the cables, and excitation level, on the performance of the control system, a parametric study is presented.

The simulations were performed on the system characterized with the parameters listed in Table 1, and ϵ_f was set at 0.5 N. The initial conditions were set at $\mathbf{x}_0$, given by Eq. (16), and the total simulation time T_s was set to 10 s. In order to study the performance of the control system under different excitation intensities, three rectangular pulses with peak acceleration (PGA) values of 25, 50, and 75 m s^{-2} were used as excitation.

In order to assess the performance of the system, the following performance indexes are introduced:

$$J_1 = \sqrt{\frac{\int_0^{T_s} |x_{s-c}(t)|^2 \, dt}{\int_0^{T_s} |x_{s-uc}(t)|^2 \, dt}}, \tag{37}$$

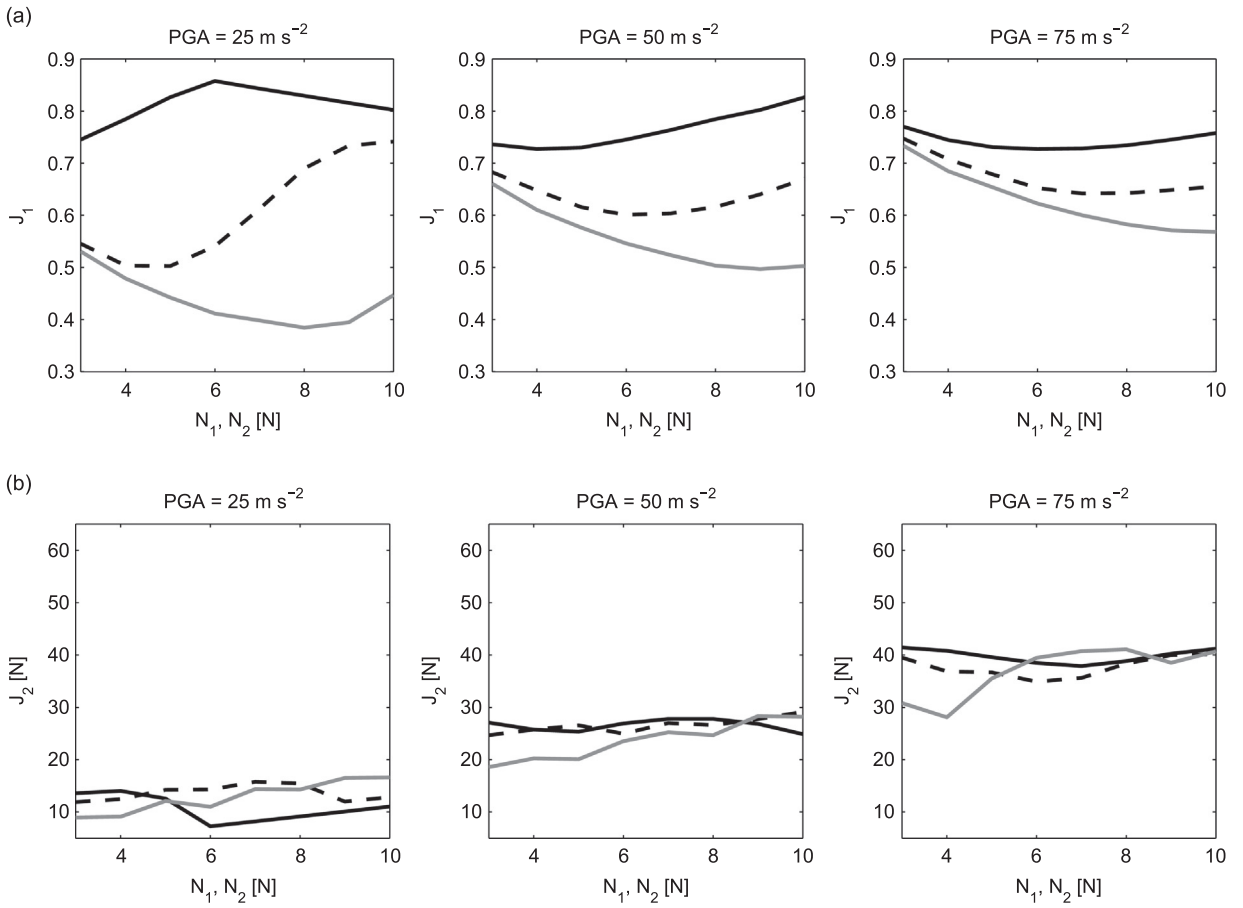

Fig. 9. Variation of the performance indexes (a) J_1 and (b) J_2 with the normal forces of the friction dampers ($N_1=N_2$), in passive mode, for the pre-tensions: $\Delta_0=0$ m (solid black line), $\Delta_0=0.010$ m (dashed black line), $\Delta_0=0.020$ m (solid grey line).

which is the ratio between the root-mean-square (RMS) value of the displacements of the controlled (x_{s-c}) and the uncontrolled (x_{s-uc}) structure, measuring the effectiveness; and

$$J_2 = \max_{0 \le t \le T_s} F_{c1}(t), \tag{38}$$

which displays the peak value of $F_{c\ 1}$ during the simulation.

6.1. Effect of the normal force in passive mode

Fig. 9a shows that the increase in the pre-tension always conduces to a reduction of the RMS value of the displacements, however from Fig. 9b it can be observed that the peak value of the cable forces does not exhibit a clear trend with the normal force or pre-tension values. From Fig. 9a, it can also be observed that the constant normal force N_i has an optimum value (which minimizes J_1); similar to the results observed by Muanke et al. [25] on a rigidly linked friction damper. In this case, the existence of the optimum value of the normal force is due to the low energy dissipation, when the normal force is small, or to the slackening of the cables, when the normal force is too large. In such cases the effectiveness is reduced. For small excitations, the following simple formula gives a good approximation of the optimum value of the normal force, and avoids the permanent slack condition:

$$N' = \frac{k_d \Delta_0}{\mu}. \tag{39}$$

6.2. Effect of the maximal normal force in semi-active mode

As Figs. 10a, 11a, and 12a demonstrate, in semi-active mode, higher maximal normal forces $N_{\max}$ always imply higher effectiveness (lower performance index J_1). This effect is less pronounced when using *Slackening-preventing law*; see Fig. 12a.

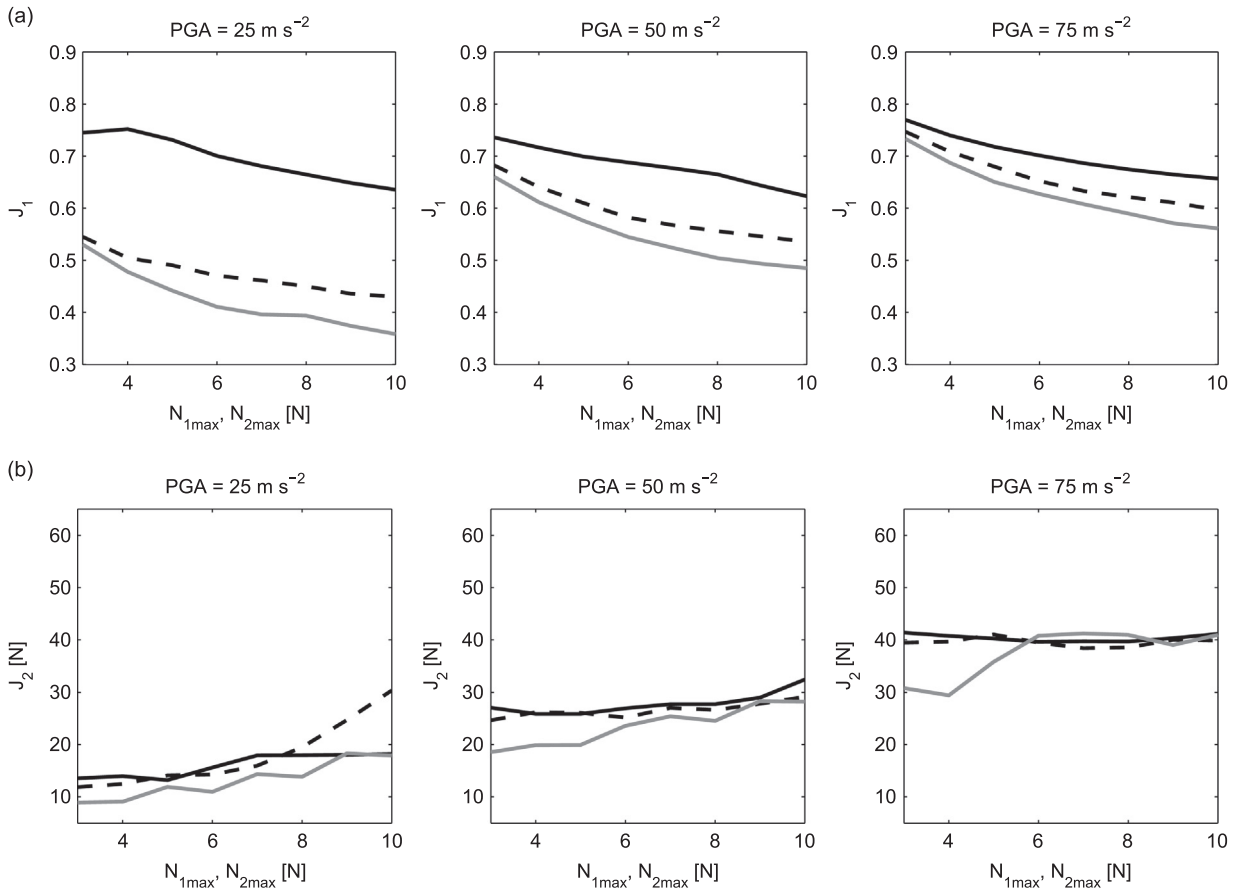

Fig. 10. Variation of the performance indexes (a) J_1 and (b) J_2 with the maximal normal forces of the friction dampers ($N_{1\max} = N_{2\max}$), with $N_{1\min} = N_{2\min} = 3$ N, in semi-active mode (*quickest-descent control law*), for the pre-tensions: Δ_0=0 m (solid black line), Δ_0=0.010 m (dashed black line), Δ_0=0.020 m (solid grey line).

It is important to note that by selecting $N_{\max}$ large enough, the control system in semi-active mode can outperform the control system in passive mode for a wide range of excitation intensities.

Similar to the passive case, the reduction in pre-tension deteriorates the effectiveness of the control system. However, this deterioration is much less in semi-active mode than in passive mode; compare Figs. 10a, 11a, and 12a with Fig. 9a. This makes the semi-active mode more reliable against loss of pre-tension (e.g., due to cable relaxation or yielding). For instance, for PGA = 25 m s^{-2}, in passive mode with $N_1 = N_2 = 8$ N and in semi-active mode (*simplified quickest-descent control law*) with $N_{1\max} = N_{2\max} = 10$ N, both with $\Delta_0 = 0.020$ m, $J_1 = 0.4$. If the cables relax 0.010 m, in passive mode $J_1 = 0.68$, whereas in semi-active mode J_1 is practically the same (0.42).

By comparing Fig. 9b to Figs. 10b, 11b, and 12b, it is observed that the peak cable forces (J_2) of the semi-active mode are similar to those of the passive mode. Fig. 10b shows that *quickest-descent control law* performs similar to passive mode in terms of J_2; whereas Figs. 11b and 12b show that, in the other control laws, larger pre-tensions lead to smaller values of J_2.

6.3. *Effect of the minimal normal force in semi-active mode*

Fig. 13a shows that, when using *quickest-descent control law*, the performance index J_1 decreases monotonically with the decrease of the minimal normal force ($N_{\min}$), being almost invariable for large pre-tensions. In the other two control laws, $N_{\min}$ have optimums, being those always less than N'. Then, as a design rule, it can be stated that $N_{\min}$ must be selected lesser or equal to N'.

In terms of J_1, the behavior of *slackening-preventing control law* is similar to that of *simplified quickest-descent control law* but J_1 depends more heavily on the pre-tension value for small values of $N_{\min}$. The latter can be explained as follows: If the normal force is set to $N_{\min}$ by the control law and the amplitude of the displacement of the structure is small enough, even when the cable is under tension, the cable force is not large enough to get over the threshold ϵ_f, remaining the normal force of the friction damper at $N_{\min}$, even though it should switch to $N_{\max}$. This weakness is mitigated by selecting a value for the parameter ϵ_f as small as practically possible.

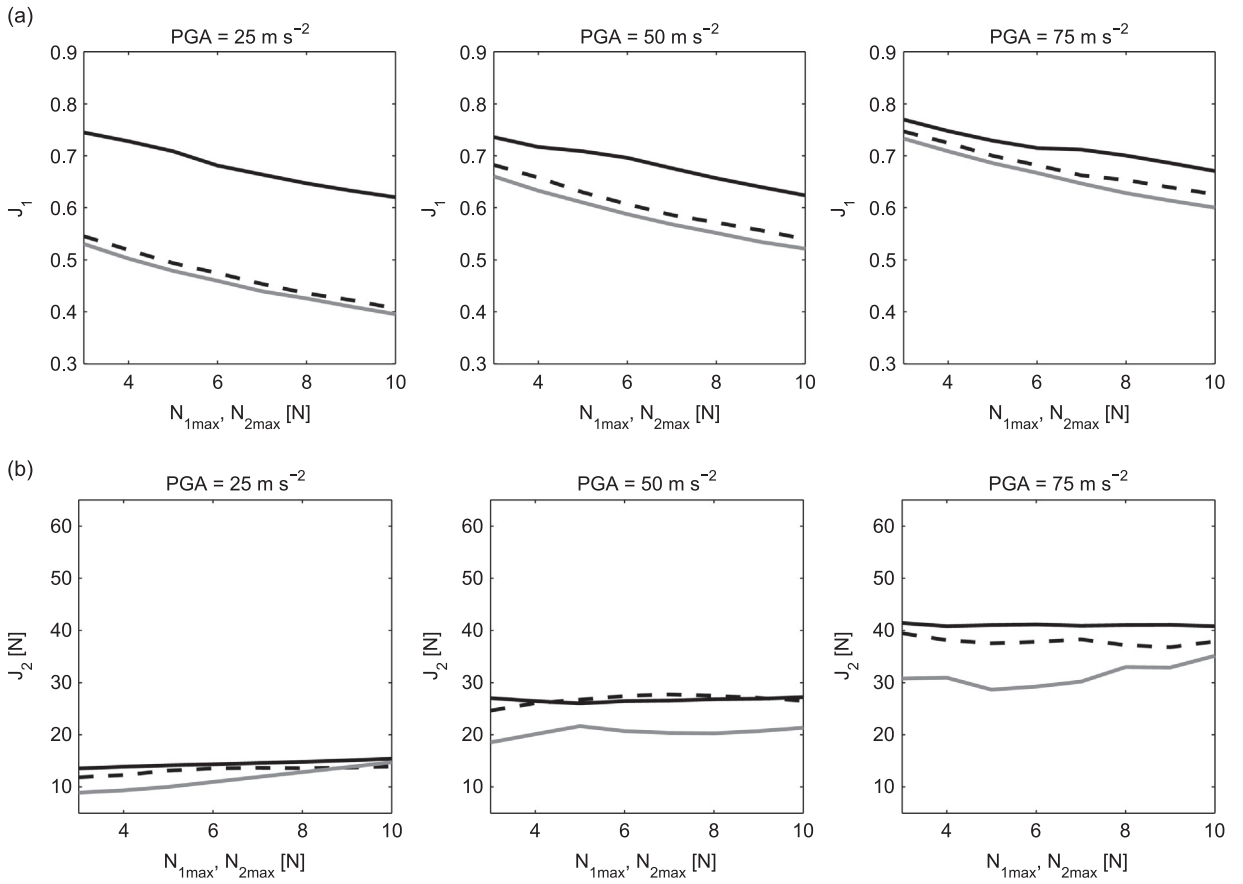

Fig. 11. Variation of the performance indexes (a) J_1 and (b) J_2 with the maximal normal forces of the friction dampers ($N_{1\max}=N_{2\max}$), with $N_{1\min}=N_{2\min}=3$ N, in semi-active mode (*simplified quickest-descent control law*), for the pre-tensions: $\Delta_0=0$ m (solid black line), $\Delta_0=0.010$ m (dashed black line), $\Delta_0=0.020$ m (solid grey line).

In *slackening-preventing control law*, when $N_{\min}$ is close to zero, J_2 results larger than those of the other two control laws; compare Figs. 13b, 14b, and 15b.

7. Application to MDOF structures

To demonstrate the performance of Semi-active Friction Tendons on actual large space structures, the SDOF structural model is extended to a structure with n DOFs, provided with m semi-active friction tendons, as shown in Fig. 16.

7.1. Equations of motion

The equations of motion of a MDOF structure can be written in matrix form as

$$\mathbf{M_s}\ddot{\mathbf{q}}_\mathbf{s}+\mathbf{C_s}\dot{\mathbf{q}}_\mathbf{s}+\mathbf{K_s}\mathbf{q_s}=(\mathbf{B_{sa}}+\mathbf{B_{sb}})\mathbf{f_c}+\mathbf{f_{es}}, \tag{40}$$

in which $\mathbf{M_s}$, $\mathbf{C_s}$, $\mathbf{K_s}$ and $\mathbf{q_s}$ are mass, damping and stiffness ($n\times n$) matrices and the vector of global coordinates, respectively. $\mathbf{B_{sa}}$ and $\mathbf{B_{sb}}$ are influence ($n\times m$) matrices of the tendons projecting the cable forces in the global coordinate system. The columns of $\mathbf{B_{sa}}$ and $\mathbf{B_{sb}}$ contain the direction cosines of ends 'a' and 'b', respectively (see Fig. 1a). The vector of cable forces $\mathbf{f_c}$ is defined as

$$\mathbf{f_c}=\mathbf{K_c}\ \mathbf{satv}(\mathbf{\Delta_0}+\mathbf{q_{da}}-\mathbf{q_d}), \tag{41}$$

where $\mathbf{K_c}$ is a ($m\times m$) diagonal matrix containing the tensile stiffness coefficients k_{ci} of each cable; **satv** is a vector function in which each element is equal to the saturation function sat defined by Eq. (4); $\mathbf{q_d}$ is a vector with the displacements of the central pads, in local coordinates; $\mathbf{\Delta_0}$ is a vector containing the pre-tension Δ_{0i} (as constant displacements) of each tendon; and $\mathbf{q_{da}}$ is a vector containing the displacements of the ends 'a' of the friction tendons, which is calculated from the

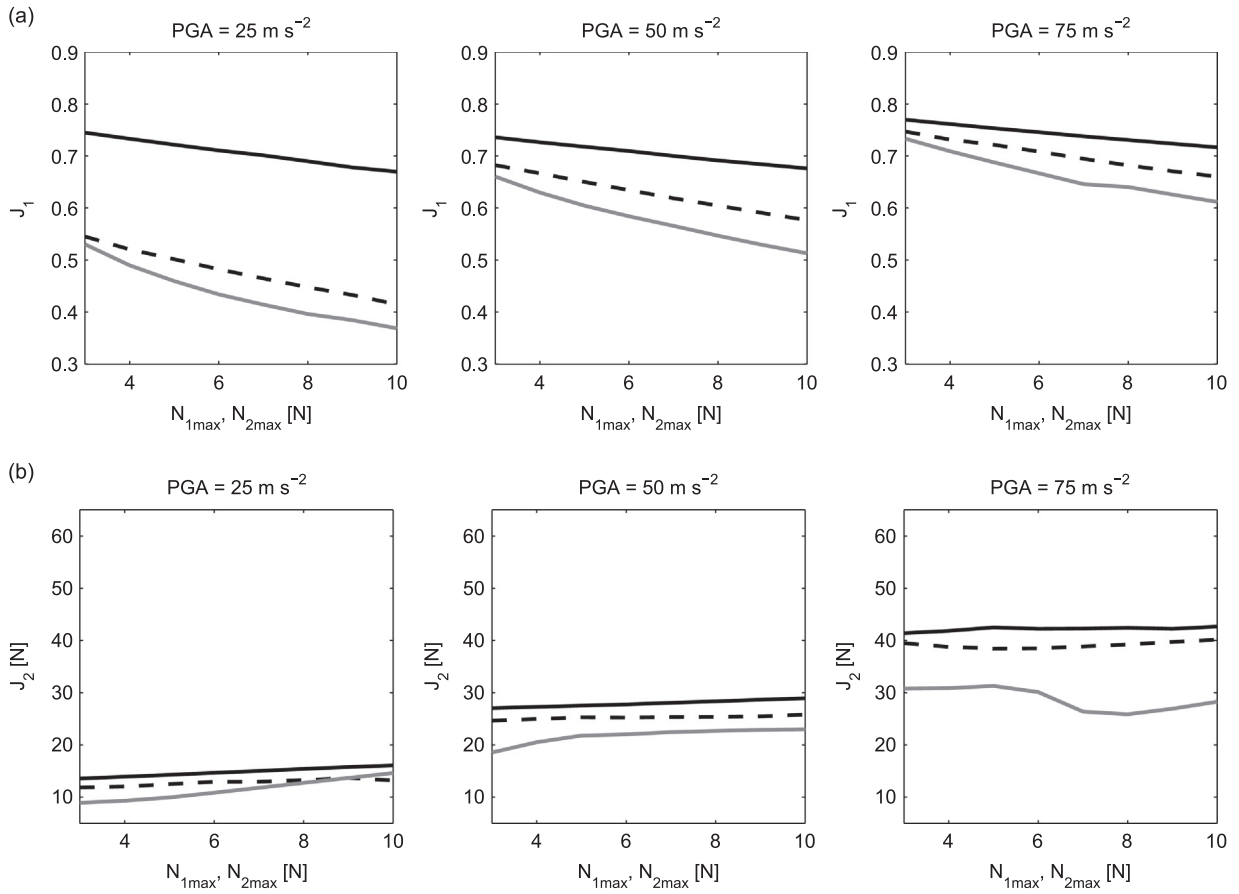

Fig. 12. Variation of the performance indexes (a) J_1 and (b) J_2 with the maximal normal forces of the friction dampers ($N_{1\max}=N_{2\max}$), with $N_{1\min}=N_{2\min}=3$ N, in semi-active mode (*slackening-preventing control law*), for the pre-tensions: Δ_0=0 m (solid black line), Δ_0=0.010 m (dashed black line), Δ_0=0.020 m (solid grey line).

displacements of the structure as

$$\mathbf{q_{da}} = -\mathbf{B_{sa}^T q_s}. \tag{42}$$

Finally, $\mathbf{f_{es}}$ is a vector of external forces on the structure, in global coordinates.

The set of semi-active friction tendons has the following (uncoupled) matrix equation of motion:

$$\mathbf{M_d}\ddot{\mathbf{q}}_\mathbf{d} + \mathbf{f_f} + \mathbf{K_d}(\mathbf{q_d} - \mathbf{q_{db}}) = \mathbf{f_c} + \mathbf{f_{ed}}, \tag{43}$$

in which $\mathbf{M_d}$ and $\mathbf{K_d}$ are $(m \times m)$ diagonal matrices which contain, respectively, the masses of the central pads m_{di} and the stiffness of the auxiliary soft springs k_{di}; $\mathbf{q_{db}}$ is a vector containing the displacements of the ends 'b' of the tendons and it is calculated from the displacements of the structure as

$$\mathbf{q_{db}} = \mathbf{B_{sb}^T q_s}. \tag{44}$$

The vector of friction-damper friction forces $\mathbf{f_f}$ is stated as

$$\mathbf{f_f} = \boldsymbol{\mu}\mathbf{N_d}\mathbf{signv}(\dot{\mathbf{q}}_\mathbf{d} - \dot{\mathbf{q}}_\mathbf{db}), \tag{45}$$

where $\boldsymbol{\mu}$ and $\mathbf{N_d}$ are $(m \times m)$ diagonal matrices which contain, respectively, the friction coefficients μ_i and the normal (variable) force N_i of the friction dampers; and **signv** is the sign vector function. Finally, $\mathbf{f_{ed}}$ is a vector of external forces on the central pads, in local coordinates.

The masses of the external pads of the friction dampers are lumped into the masses of the corresponding DOFs of the structure.

For a free–free structure (such as the space structures) in which the rigid body modes were removed by adding "dummy constraints" [21], the external forces can be calculated as follows:

$$\mathbf{f'_{es}} = \mathbf{f'_{esf}} - \mathbf{M'_s}\boldsymbol{\Phi}_\mathbf{r}\ddot{\mathbf{q}}_\mathbf{g}, \quad \mathbf{f}_{ed} = -\mathbf{M_d}\mathbf{B'_{sb}}^{\mathbf{T}}\boldsymbol{\Phi}_\mathbf{r}\ddot{\mathbf{q}}_\mathbf{g}, \tag{46}$$

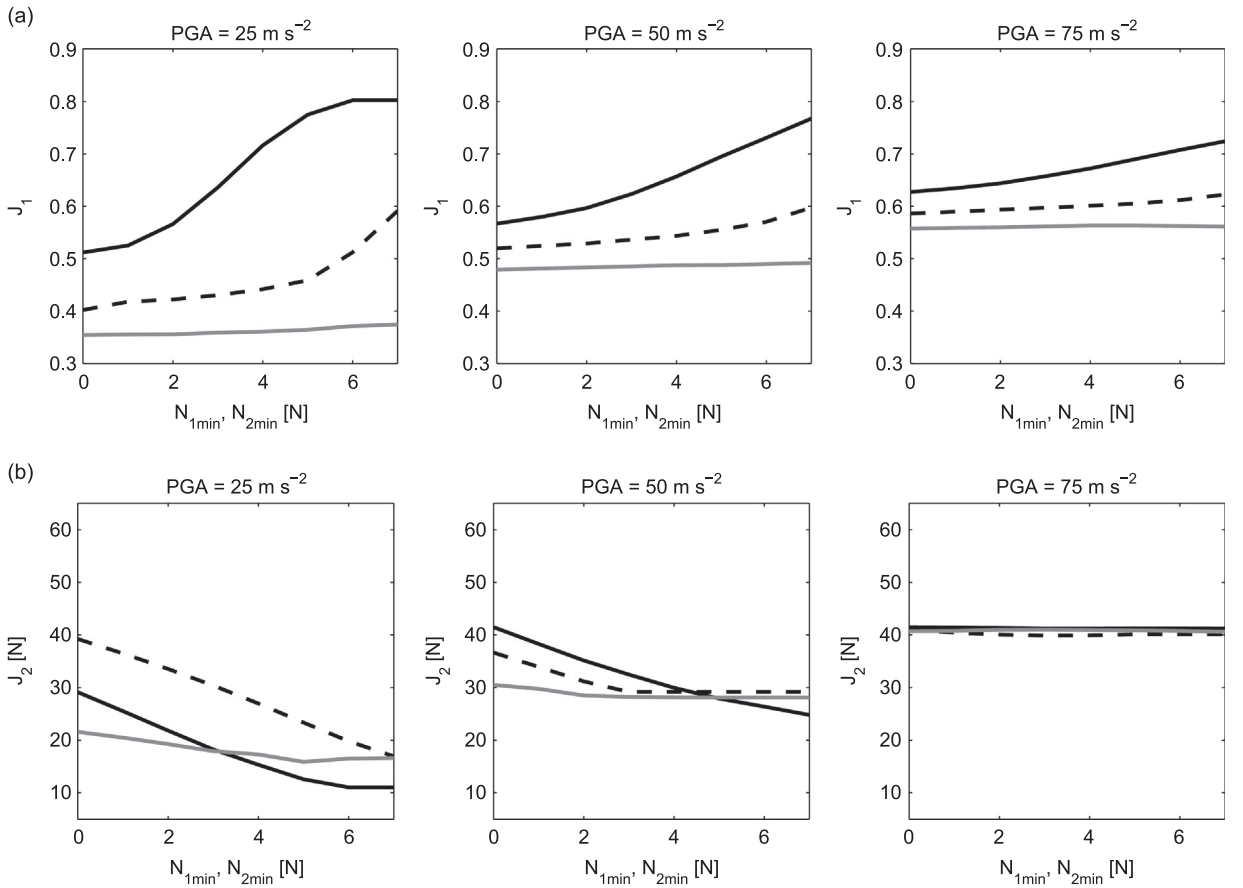

Fig. 13. Variation of the performance indexes (a) J_1 and (b) J_2 with the minimal normal forces of the friction dampers ($N_{1\min}=N_{2\min}$), with $N_{1\max}=N_{2\max}=10$ N, in semi-active mode (*quickest-descent control law*), for the pre-tensions: $\Delta_0=0$ m (solid black line), $\Delta_0=0.010$ m (dashed black line), $\Delta_0=0.020$ m (solid grey line).

in which $\mathbf{f}'_{\mathbf{esf}}$ is the vector of actual external forces applied to the free–free structure (which has rigid body modes), $\mathbf{\Phi_r}$ is a matrix containing the (up to 6) rigid body modes as columns, $\mathbf{M}'_{\mathbf{s}}$ and $\mathbf{B}'_{sb}$ are the mass and the influence matrices of the structure with rigid body modes ($\mathbf{M_s}$ and $\mathbf{B_{sb}}$ are obtained from those by removing the elements corresponding to the "dummy constraints"), and $\ddot{\mathbf{q}}_{\mathbf{g}}$ is a vector of (up to 6) rigid body accelerations (support accelerations) which can be calculated as [21] (neglecting the masses of the friction dampers)

$$\ddot{\mathbf{q}}_{\mathbf{g}}=(\mathbf{\Phi}_{\mathbf{r}}^{\mathbf{T}}\mathbf{M}'_{\mathbf{s}}\mathbf{\Phi}_{\mathbf{r}})^{-1}\mathbf{\Phi}_{\mathbf{r}}^{\mathbf{T}}\mathbf{f}_{\mathbf{esf}}{}'. \tag{47}$$

Then, $\mathbf{f_{es}}$ is obtained from $\mathbf{f}'_{\mathbf{es}}$ by removing the elements corresponding to the "dummy constraints".

7.2. Example structure and excitation

The free–free aluminium truss shown in Fig. 16 was adopted to assess the effectiveness of the semi-active friction tendons for controlling the vibration of their arms. The structure, whose principal geometrical characteristics can be found in [23], is representative of the Micro-Precision Interferometer JPL-MPI [21].

The mass and stiffness matrices $\mathbf{M_s}$ and $\mathbf{K_s}$ of the 233 DOFs model [23] with "dummy constrains" in the central corner were obtained from a commercial finite element software package. The matrix $\mathbf{C_s}$ was chosen to provide a damping ratio of 1 percent to the first mode. The first three natural frequencies were found to be 7.03 Hz, 9.23 Hz, and 14.17 Hz.

According to the type of excitation to which a space structure may be subjected (as an extreme case), an artificially generated white-noise force record of 20 s duration, with an RMS value equal to 100 N in the direction of each arm, was applied to the central corner of the structure.

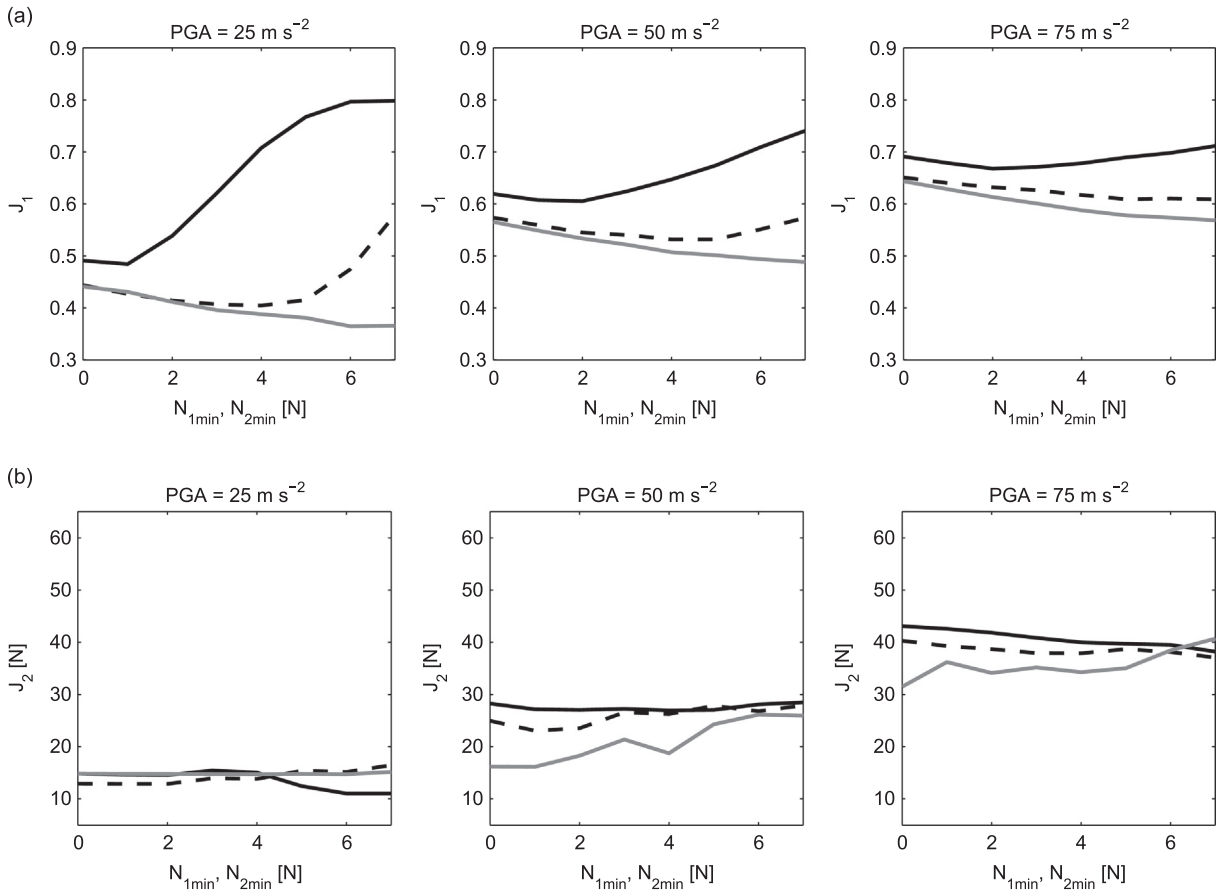

Fig. 14. Variation of the performance indexes (a) J_1 and (b) J_2 with the minimal normal forces of the friction dampers ($N_{1\min}=N_{2\min}$), with $N_{1\max}=N_{2\max}=10$ N, in semi-active mode (*simplified quickest-descent control law*), for the pre-tensions: Δ_0=0 m (solid black line), Δ_0=0.010 m (dashed black line), Δ_0=0.020 m (solid grey line).

7.3. Vibration control system

The friction tendons were designed as follows. Three light 3.16 mm diameter cables, made of "Dyneema" synthetic fiber (EA=180 000 N) [23], of 6.84 m, 8.53 m and 7.82 m length, were connected to friction dampers with $\mu=0.5$, $N_{\min}=1$ N, $N_{\max}=20$ N, $m_d=0.05$ kg, and to auxiliary springs with $k_d=200$ N m^{-1}, as shown in Fig. 16.

From a preliminary dynamic analysis of the uncontrolled case, it was found an upper bound for the displacements between the nodes in which the tendons were installed equal to $x_{s\max}=0.003$ m (corresponding to RMS displacements equal to 0.0014 m, for Tendon 1). Besides, it was assumed that the static deformation of the structure due to the pre-tension of the tendons must be lower than 10 percent of $x_{s\max}$ (e.g. by limiting the static cable forces to 2 N). Then, each pre-tension value Δ_0 was chosen to be equal to 0.01 m; which satisfies (1) the necessary condition (B.8) (i.e., $\Delta_0 > x_{s\max}$) and (2) the static design constraints (i.e., $k_d\Delta_0=2$ N). Note also that for $N_{\min}=1$ N, condition (B.7) holds (neglecting $f_{ed\max}$), i.e. cables are always taut.

For the control system working in semi-active mode, a decentralized approach was used to provide collocated damping to the structure between their arms. The three normal forces were considered to be variable between $N_{\min}$ and $N_{\max}$ according to the *simplified quickest descent control law* stated in Eq. (30), but using the tendon relative velocities $\dot{\mathbf{q}}_{\mathbf{da}}-\dot{\mathbf{q}}_{\mathbf{db}}$ instead of the (SDOF) structure velocity $\dot{x}_s$.

Four cases of the control system working in passive mode were studied as a baseline for comparison. The normal forces (N) were considered to be constant at: (1) 1 N, i.e. the normal force which corresponds to $N_{\min}$, (2) 20 N, i.e. the normal force which corresponds to $N_{\max}$, (3) 4 N, i.e. the maximal normal force which satisfies condition (B.9) (i.e. prevention of permanent slackening), and (4) 2.8 N, i.e. the maximal normal force which satisfies condition (B.7) (i.e. cables are always taut). This last value is also the optimal normal force for the passive mode.

7.4. Results and discussion

The tendon displacements $\mathbf{q}_{\mathbf{da}}-\mathbf{q}_{\mathbf{db}}$ (i.e., the displacements between the nodes of the structure in which the tendons are placed), the friction damper displacements $\mathbf{q}_{\mathbf{d}}-\mathbf{q}_{\mathbf{db}}$ (i.e., the deformations of the auxiliary soft springs), and the cable forces

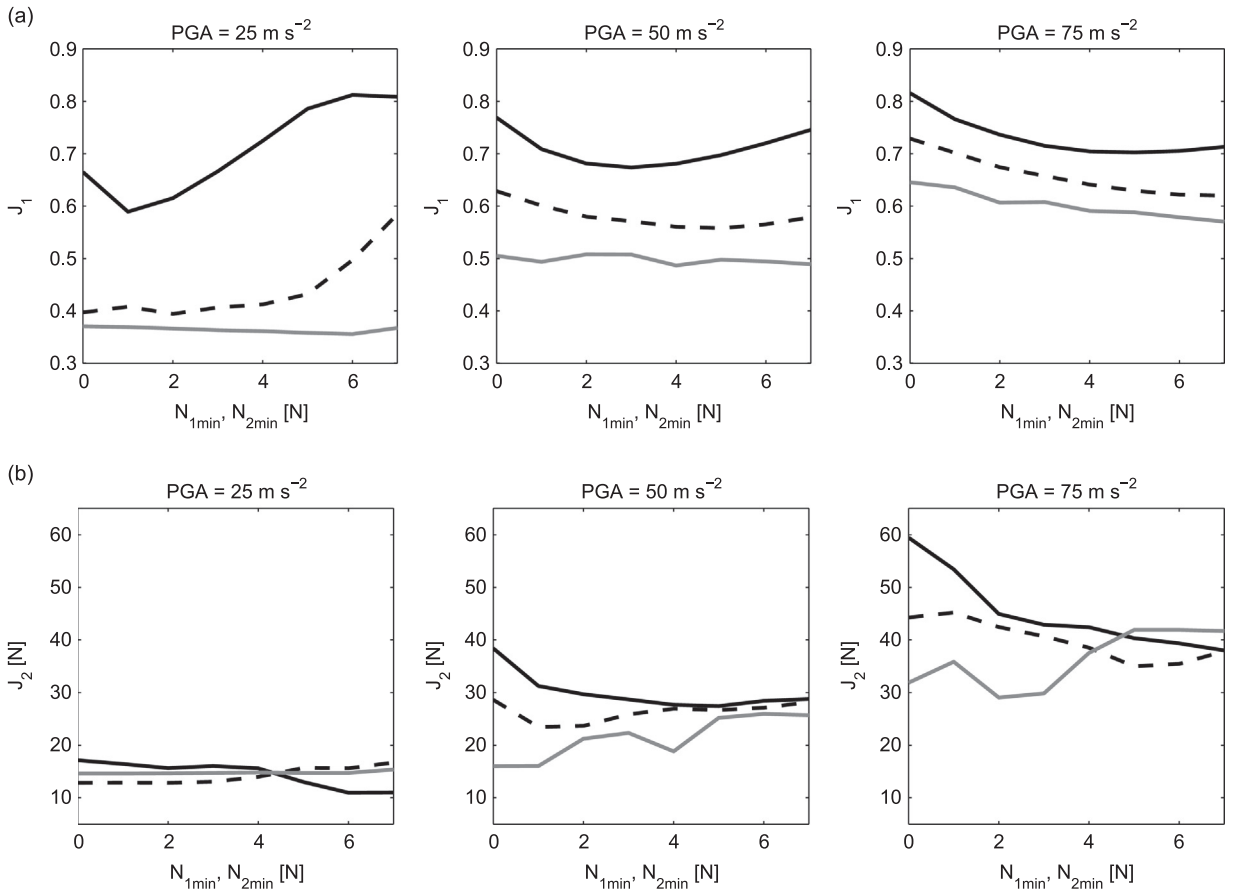

Fig. 15. Variation of the performance indexes (a) J_1 and (b) J_2 with the minimal normal forces of the friction dampers ($N_{1\min}=N_{2\min}$), with $N_{1\max}=N_{2\max}=10$ N, in semi-active mode (*slackening-preventing control law*), for the pre-tensions: $\Delta_0=0$ m (solid black line), $\Delta_0=0.010$ m (dashed black line), $\Delta_0=0.020$ m (solid grey line).

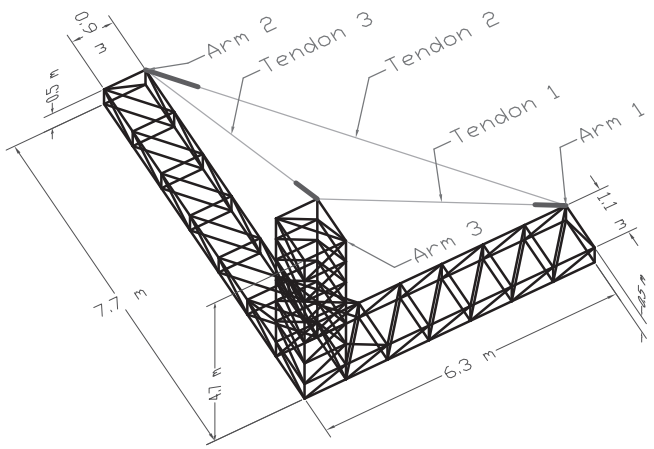

Fig. 16. Structure which is representative of the JPL-MPI, with three semi-active friction tendons. Thick lines indicate parallel arrangements of auxiliary spring and friction damper.

$\mathbf{f_c}$ were studied. These responses are shown in Figs. 17–20 for passive mode, and in Fig. 21 for semi-active mode. The effectiveness in controlling the structure displacements ($\mathbf{q_{da}}-\mathbf{q_{db}}$) was assessed in terms of the performance index J_1, stated in Eq. (37), for Tendon 1 (i.e. the RMS values of $q_{da1}-q_{db1}$).

As shown in Figs. 17 ($N=1$ N) and 18 ($N=20$ N), normal forces which are too low or too high lead to poor effectiveness (J_1 is equal to 0.80 and 0.96, respectively). Besides, from the damper displacements shown in Fig. 18 ($N=$ 20 N), it is observed that the friction dampers do not return to the initial positions after slide.

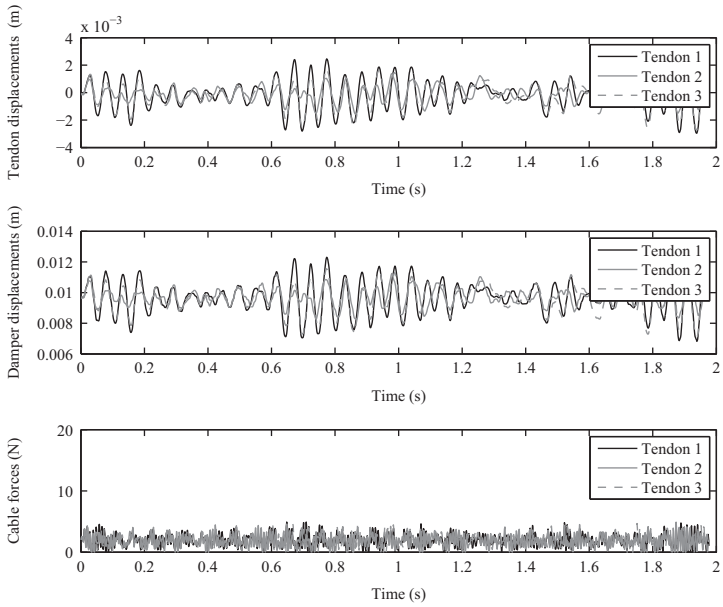

Fig. 17. Responses of the controlled structure in passive mode with normal forces equal to 1 N.

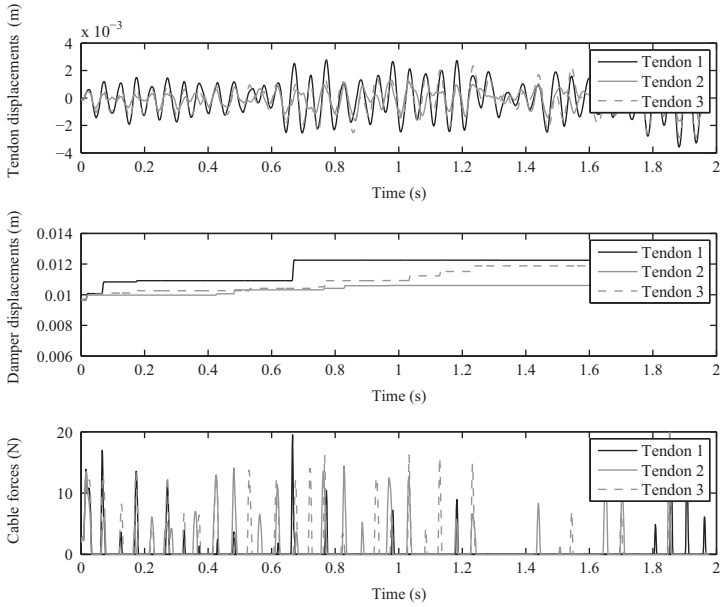

Fig. 18. Responses of the controlled structure in passive mode with normal forces equal to 20 N.

For the case shown in Fig. 19 (N=4 N), the friction dampers return to the initial positions after each slide (see damper displacements); however, cables are not always taut (see cable forces). This case shows tendon displacement lower ($J_1 = 0.65$) than cases of N=1 N and N=20 N.

Finally, as can be seen in Fig. 20 (N=2.8 N), the best performance is achieved by using the higher normal force which ensures that cables are always taut ($J_1 = 0.61$).

The responses of the control system in semi-active mode are shown in Fig. 21. The effectiveness is better ($J_1 = 0.41$) than that of the optimal passive case ($J_1 = 0.61$, for N=2.8 N). Note that cable forces are as high as in the passive case of N=20 N, while cables are always taut as in the passive cases of N=1 N and 2.8 N.

It is also important to highlight that, although semi-active friction tendons are not placed as symmetric pairs, they can reduce (with a non symmetrical response) both the positive and the negative peaks of tendon displacements considerably (see Fig. 21); due to energy dissipation.

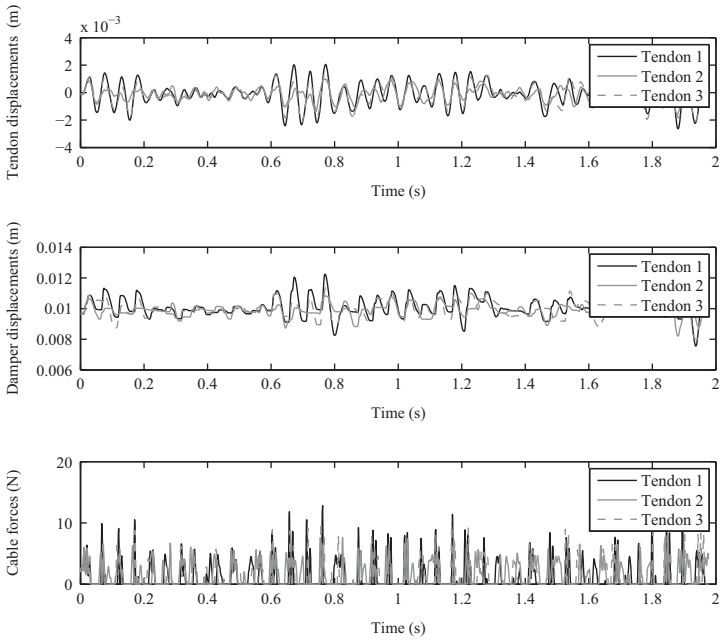

Fig. 19. Responses of the controlled structure in passive mode with normal forces equal to 4 N.

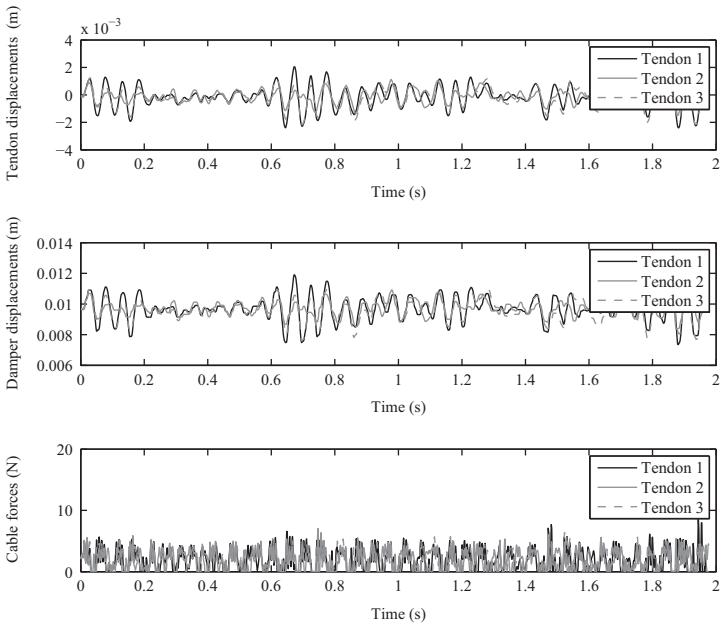

Fig. 20. Responses of the controlled structure in passive mode with normal forces equal to 2.8 N.

8. Conclusions

A semi-active cable-based vibration control system, using dry-fiction dampers, has been proposed and studied in some detail. Using cables makes the system suitable for deployable and light-weight structures, such as the (large) space structures. Cables are held taut by means of auxiliary soft springs placed in parallel with the friction dampers, and an appropriate semi-active control law. The system can work in passive mode (i.e. constant normal forces) or semi-active mode (i.e. normal forces are smartly adjusted in real time). Three semi-active control laws, named *quickest-descent control law*, *simplified quickest-descent control law*, and *slackening-preventing control law*, have been proposed and studied.

The main advantage of semi-active- over passive-mode, in which it is based on its high effectiveness and reliability, is the ability to change the normal force between a minimum value, to avoid the slackening of the cables, and a maximum to increase the energy dissipation.

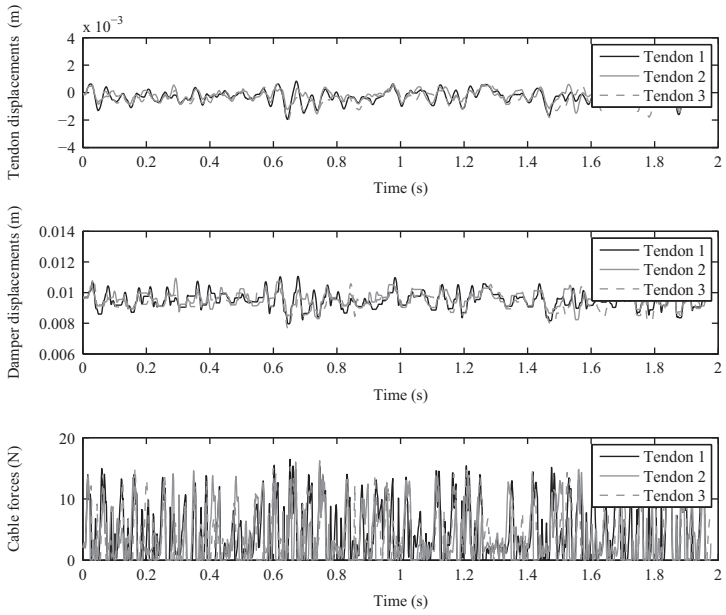

Fig. 21. Responses of the controlled structure in semi-active mode with normal forces variable between 1 N and 20 N.

In order to assess the effect of the normal force of the friction dampers and the pre-tension of the cables on the effectiveness of the control system, a parametric study was carried out on a SDOF model. The study showed that the decrease in pre-tension deteriorates the effectiveness in all the cases studied. However, the semi-active mode is less sensitive to that change; and therefore it is more reliable.

Any control law studied in this work provides good effectiveness to the control system. Particularly, the *simplified quickest-descent control law* and the *slackening-preventing control law* display lower frequencies in the command signals, whereas the *quickest-descent control law* takes more advantage of the small values of the minimal normal force.

It was outlined an application of the developed vibration control method to a MDOF structure through a decentralized- and collocated-approach. The performance of the control system was good in both passive- and semi-active-modes. However, as in SDOF systems, semi-active mode was more effective than the optimal passive case.

Finally it should be underlined that, although the proposed system is especially suitable for flexible structures such as those with high restrictions in volume and weight, it can also be applied to civil and mechanical structures.

Acknowledgments

The authors would like to express their thanks to CONICET and National University of Cuyo for the financial support. Special acknowledgments are extended to the reviewers of the first version of the paper, since their useful recommendations led to substantial improvements of the final version of the paper.

Appendix A. Equilibrium point of the system

A vector $\mathbf{x}_0$ is an equilibrium point of the system (11) if [30]

$$\mathbf{f}(\mathbf{x}_0) = \mathbf{0}, \tag{A.1}$$

where $\mathbf{x}_0 = [x_{s0}\ x_{d10}\ x_{d20}\ \dot{x}_{s0}\ \dot{x}_{d10}\ \dot{x}_{d20}]^{\mathbf{T}}$, and $\mathbf{0} = [0\ 0\ 0\ 0\ 0\ 0]^{\mathbf{T}}$.

Considering the expressions (13) and (15), (A.1) can be written as

$$\begin{bmatrix} \dot{x}_{s0} \\ \dot{x}_{d10} \\ \dot{x}_{d20} \\ \frac{1}{m_s}\left(-k_s x_{s0} - c_s \dot{x}_{s0} - k_c\ \mathrm{sat}(x_{s0} - x_{d10} + \Delta_0) + k_c\ \mathrm{sat}(-x_{s0} + x_{d20} + \Delta_0)\right) \\ \frac{1}{m_d}\left(-k_d x_{d10} - \mu N_1\ \mathrm{sgn}(\dot{x}_{d10}) + k_c\ \mathrm{sat}(x_{s0} - x_{d10} + \Delta_0)\right) \\ \frac{1}{m_d}\left(-k_d x_{d20} - \mu N_2\ \mathrm{sgn}(\dot{x}_{d20}) - k_c\ \mathrm{sat}(-x_{s0} + x_{d20} + \Delta_0)\right) \end{bmatrix} = \begin{bmatrix} 0 \\ 0 \\ 0 \\ 0 \\ 0 \\ 0 \end{bmatrix}. \tag{A.2}$$

And, since $\mathrm{sgn}(0)=0$, it follows that

$$\begin{bmatrix} -k_s x_{s0} - c_s \dot{x}_{s0} - k_c\ \mathrm{sat}(x_{s0} - x_{d10} + \Delta_0) + k_c\ \mathrm{sat}(-x_{s0} + x_{d20} + \Delta_0) \\ -k_d x_{d10} - \mu_1 N_1 + k_c\ \mathrm{sat}(x_{s0} - x_{d10} + \Delta_0) \\ -k_d x_{d20} - \mu_2 N_2 - k_c\ \mathrm{sat}(-x_{s0} + x_{d20} + \Delta_0) \end{bmatrix} = \begin{bmatrix} 0 \\ 0 \\ 0 \end{bmatrix}. \tag{A.3}$$

Considering $\Delta_0 \geq 0$, the following assumptions can be introduced:

$$x_{s0} - x_{d10} + \Delta_0 \geq 0, \tag{A.4}$$

$$-x_{s0} + x_{d20} + \Delta_0 \geq 0, \tag{A.5}$$

through which Eq. (A.3) yields the following system of linear equations (in matrix form):

$$\begin{bmatrix} k_s + 2k_c & -k_c & -k_c \\ k_c & -k_d - k_c & 0 \\ k_c & 0 & -k_d - k_c \end{bmatrix} \begin{bmatrix} x_{s0} \\ x_{d10} \\ x_{d20} \end{bmatrix} = \begin{bmatrix} 0 \\ -k_c \Delta_0 \\ k_c \Delta_0 \end{bmatrix}, \tag{A.6}$$

whose unique solution is

$$\begin{bmatrix} x_{s0} \\ x_{d10} \\ x_{d20} \end{bmatrix} = \frac{k_c \Delta_0}{k_c + k_d} \begin{bmatrix} 0 \\ 1 \\ -1 \end{bmatrix}. \tag{A.7}$$

For the equilibrium state, $\dot{x}_{s0} = \dot{x}_{d10} = \dot{x}_{d20} = 0$, i.e. all the masses are in response; the equilibrium deformations of auxiliary springs are symmetrically opposed ($x_{d10} = -x_{d20}$) and do not depend on the stiffness of the structure; and $x_{s0} = 0$, i.e. the equilibrium position of the structure is not changed after the installation of the tendons.

Finally, since k_d is positive-definite, from expression (A.7) it can be easily shown that the assumptions (A.4) and (A.5) are valid if $\Delta_0 \geq 0$.

Appendix B. Lyapunov stability analysis assuming bounded input

A simplified analysis of the Lyapunov stability is made for the system shown in Fig. 2 under bounded excitation. This analysis provides sufficient (but not necessary) conditions for ultimate boundedness (total stability, [31]) of the controlled-system velocity response (for both *modes*, *semi-active* and *passive*), and the value of the ultimate bound as a function of the main design parameters of the vibration control system and the bounds of external forces. First, the stability analysis is made for semi-active control. Then, passive control is studied as a particular case of semi-active control.

The following assumptions are made:

1. Input forces are bounded, i.e. $|f_{es}| < f_{es\max}, |f_{ed1}| < f_{ed\max}, |f_{ed2}| < f_{ed\max}$.
2. Maximum structure response is bounded, i.e. $|x_s| < x_{s\max}, |\dot{x}_s| < v_{s\max}$.
3. Structural damping ratio is very low but not zero, i.e. $0 < c_s \ll 2\omega_s m_s$, being $\omega_s = \sqrt{k_s/m_s}$.
4. The cables are always taut, i.e. $F_{c1} > 0, F_{c2} > 0$.
5. Since cables are always taut and cable stiffness are very large as compared to auxiliary-springs stiffness, i.e. $k_{c1} \gg k_{d1}, k_{c2} \gg k_{d2}$, then $x_{d1} \approx x_s + \Delta_0, x_{d2} \approx x_s - \Delta_0$. This assumption leads to the following.
6. Signs of velocities are equal most of the time, i.e. $\mathrm{sgn}(\dot{x}_s) \approx \mathrm{sgn}(\dot{x}_{di})$ for $i = 1, 2$.
7. Inertial forces in the friction dampers, due to relative accelerations, are negligible as compared to frictional forces, i.e. $m_d \ddot{x}_{d1} \approx 0, m_d \ddot{x}_{d2} \approx 0$. Note that $\ddot{x}_{d1}$ and $\ddot{x}_{d2}$ do not include support (rigid body) acceleration, which is taken into account by $f_{ed\ 1}$ and $f_{ed\ 2}$.

Assuming these considerations, the cable forces can be approximately stated as

$$F_{c1} \approx k_d(x_s + \Delta_0) + \mu N_1 \mathrm{sgn}(\dot{x}_s) - f_{ed1}, \tag{B.1}$$

$$F_{c2} \approx -k_d(x_s - \Delta_0) - \mu N_2 \mathrm{sgn}(\dot{x}_s) + f_{ed2}, \tag{B.2}$$

from which sufficient conditions can be stated in order to ensure that cables are always taut.

First, consider the case in which $\dot{x}_s > 0$. Applying control law (27), or (30) and (31), to approximations (B.1) and (B.2) yields

$$F_{c1} \approx k_d(x_s + \Delta_0) + \mu N_{1\max} - f_{ed1} \quad \text{if } \dot{x}_s > 0, \tag{B.3}$$

$$F_{c2} \approx -k_d(x_s - \Delta_0) - \mu N_{2\min} + f_{ed2} \quad \text{if } \dot{x}_s > 0. \tag{B.4}$$

In the same way, considering the case in which $\dot{x}_s < 0$ yields

$$F_{c1} \approx k_d(x_s + \Delta_0) - \mu N_{1\min} - f_{ed1} \quad \text{if } \dot{x}_s < 0, \tag{B.5}$$

$$F_{c2} \approx -k_d(x_s - \Delta_0) + \mu N_{2\max} + f_{ed2} \quad \text{if } \dot{x}_s < 0. \tag{B.6}$$

From expressions (B.3)–(B.6), the following sufficient condition can be found to ensure that $F_{c1} > 0$ and $F_{c2} > 0$ hold always (no slackening):

$$\max_{i=1,2} \mu N_{i\min} < k_d(\Delta_0 - x_{s\max}) - f_{ed\max}. \tag{B.7}$$

For $\dot{x}_s = 0$, condition (B.7) is still sufficient to ensure that both cables are always taut. An important fact is that $N_{1\max}$ and $N_{2\max}$ do not appear in condition (B.7).

Condition (B.7) has the following important corollary which can be used in pre-design:

$$\Delta_0 > x_{s\max}. \tag{B.8}$$

If the external forces on the friction dampers are neglected, condition (B.7) can be relaxed as

$$\max_{i=1,2} \mu N_{i\min} < k_d \Delta_0, \tag{B.9}$$

which only ensures that at least one of the two cables is taut, and the cables never enter in a condition of permanent slackening. This can be useful in pre-design but do not ensures maximum effectiveness in control.

Now, considering for simplicity $N_{1\min} = N_{2\min} = N_{\min}$ and $N_{1\max} = N_{2\max} = N_{\max}$, previously stated assumptions and expressions (B.3), (B.4), (B.5) and (B.6) can be used to approximate Eq. (26) as

$$\dot{V}(\mathbf{z}) \approx -c_s\dot{x}_s^2 + \dot{x}_s(-k_d(x_s - \Delta_0) + f_{ed2} - k_d(x_s + \Delta_0) - \operatorname{sgn}(\dot{x}_s)\mu(N_{\max} + N_{\min}) + f_{ed1}) + \dot{x}_s f_{es} + 2k_d x_s \dot{x}_s, \tag{B.10}$$

which can be rewritten as

$$\dot{V}(\mathbf{z}) \approx -c_s\dot{x}_s^2 - |\dot{x}_s|\mu(N_{\max} + N_{\min}) + \dot{x}_s(f_{ed2} + f_{ed1} + f_{es}), \tag{B.11}$$

and

$$\dot{V}(\mathbf{z}) \lessapprox -c_s|\dot{x}_s|^2 + |\dot{x}_s|(2f_{ed\max} + f_{es\max} - \mu(N_{\max} + N_{\min})), \tag{B.12}$$

which leads to the following statement:

$$\text{if} \quad |\dot{x}_s| > v_{s\max} \quad \text{then } \dot{V}(\dot{x}_s) \lessapprox 0, \tag{B.13}$$

where

$$v_{s\max} = \frac{2f_{ed\max} + f_{es\max} - \mu(N_{\max} + N_{\min})}{c_s}. \tag{B.14}$$

This means that the interval $(-v_{s\max}, v_{s\max})$ provides a stable attractor (ultimate bound [31]) for the velocity of the structure under bounded excitation on the assumption that condition (B.7) holds (which is sufficient but not necessary). Note that this velocity bound can be as small as desired only by increasing $N_{\max}$, while condition (B.7) can be hold for any displacement (assuming (B.8) holds and external forces on the friction dampers are small) only by decreasing $N_{\min}$.

Another important corollary of Eq. (B.14) is that the ultimate bound can be reduced by reducing the bounds of external forces applied on the structure and on the masses of the friction dampers. The first bound ($f_{es\max}$) is usually a design constraint while the second one ($f_{ed\max}$) can be reduced by reducing the masses of the friction dampers, if external forces in friction dampers are inertial only.

In case of passive control, $N_{\min} = N_{\max} = N$. Then, the velocity ultimate bound can be as small as desired by increasing N only up to the point in which condition (B.7) does not hold.

For values of $N_{i\min}$ such that condition (B.7) is not satisfied, the velocity ultimate bound cannot be predicted through this simplified analysis.

References

[1] M. Moshrefi-Torbati, A.J. Keane, S.J. Elliott, M.J. Brennan, E. Rogers, Passive vibration control of a satellite boom structure by geometric optimization using genetic algorithm, *Journal of Sound and Vibration* 267 (4) (2003) 879–892, http://dx.doi.org/10.1016/S0022-460X(03)00192-5.

[2] F. Dignath, W. Schiehlen, Control of the vibrations of a tethered satellite system, *Journal of Applied Mathematics and Mechanics* 64 (5) (2000) 715–722, http://dx.doi.org/10.1016/S0021-8928(00)00100-3.

[3] T.T. Soong and G.F. Dargush, Passive Energy Dissipation Systems in Structural Engineering, John Wiley & Sons, Chichester, UK, 1997, http://dx.doi.org/10.1002/stc.4300060114.

[4] F. Naeim and J.M. Kelly, Design of Seismic Isolated Structures: From Theory to Practice, John Wiley & Sons, New York, US, 1999, http://dx.doi.org/10.1002/9780470172742.

[5] A. Preumont, K. Seto, *Active Control of Structures*, John Wiley & Sons, Chichester, UK, 2008.

[6] M. Azadi, S. Fazelzadeh, M. Eghtesad, E. Azadi, Vibration suppression and adaptive-robust control of a smart flexible satellite with three axes maneuvering, *Acta Astronautica* 69 (5–6) (2011) 307–322, http://dx.doi.org/10.1016/j.actaastro.2011.04.001.

[7] F. Casciati, G. Magonette, F. Marazzi, *Technology of Semiactive Devices and Applications in Vibration Mitigation*, John Wiley & Sons, Ltd, Chichester, UK http://dx.doi.org/10.1002/0470022914.

[8] K. Makihara, J. Onoda, M. Tsuchihashi, Investigation of performance in suppressing various vibrations with energy-recycling semi-active method, *Acta Astronautica* 58 (10) (2006) 506–514, http://dx.doi.org/10.1016/j.actaastro.2006.01.007.
[9] M.J. Balas, Trends in large space structure control theory: *fondest hopes, wildest dreams*, *IEEE Transactions on Automatic Control* 27 (3) (1982) 522–535, http://dx.doi.org/10.1109/TAC.1982.1102953.
[10] G. Tibert, Deployable Tensegrity Structures for Space Applications, PhD Thesis, Royal Institute of Technology, 2002.
[11] A.A. Golafshani, E.K. Rahani, M.R. Tabeshpour, A new high performance semi-active bracing system, *Engineering Structures* 28 (14) (2006) 1972–1982, http://dx.doi.org/10.1016/j.engstruct.2006.03.032.
[12] E.K. Rahani, A. Bakhshi, A.A. Golafshani, Semiactive Viscous Tensile Bracing System, *Journal of Structural Engineering* 135 (4) (2009) 425–436, http://dx.doi.org/10.1061/(ASCE)0733-9445(2009)135:4(425).
[13] J. Mitsugi, Static analysis of cable networks and their supporting structures, *Computers & Structures* 51 (1) (1994) 47–56.
[14] H.M. Irvine, *Cable Structures, The MIT Press Series in Structural Mechanics*, MIT Press, Cambridge, MA, London, England, 1992.
[15] E. Guevara, G. McClure, Nonlinear seismic response of antenna-supporting structures, *Computers & Structures* 47 (4/5) (1993) 711–724.
[16] F. Casciati, F. Ubertini, Nonlinear vibration of shallow cables with semiactive tuned mass damper, *Nonlinear Dynamics* 53 (1–2) (2007) 89–106, http://dx.doi.org/10.1007/s11071-007-9298-y.
[17] O. Lopez-Garcia, A. Carnicero, V. Torres, J. Jimenez-Octavio, The influence of cable slackening on the stiffness computation of railway overheads, *International Journal of Mechanical Sciences* 50 (7) (2008) 1213–1223, http://dx.doi.org/10.1016/j.ijmecsci.2008.04.001.
[18] G.F. Giaccu, L. Caracoglia, Generalized power-law stiffness model for nonlinear dynamics of in-plane cable networks, *Journal of Sound and Vibration* 332 (8) (2013) 1961–1981, http://dx.doi.org/10.1016/j.jsv.2012.12.006.
[19] K. Lee, J. Chung, Dynamic analysis of a hanger-supported beam with a moving oscillator, *Journal of Sound and Vibration* 332 (13) (2013) 3177–3189, http://dx.doi.org/10.1016/j.jsv.2013.01.015.
[20] Z. Wang, T. Li, Y. Cao, Active shape adjustment of cable net structures with PZT actuators, *Aerospace Science and Technology* 26 (1) (2013) 160–168, http://dx.doi.org/10.1016/j.ast.2012.03.001.
[21] A. PREUMONT, *Vibration Control of Active Structures: An Introduction*, 3rd ed. Springer, New York, Boston, Dordrecht, London, Moscowhttp://dx.doi.org/10.1007/978-94-007-2033-6 Library.
[22] M. Smrz, R. Bastaits, A. Preumont, Active damping of the camera support mast of a Cherenkov Gamma-ray telescope, *Nuclear Instruments and Methods in Physics Research Section A: Accelerators, Spectrometers, Detectors and Associated Equipment* 635 (1) (2011) 44–52, http://dx.doi.org/10.1016/j.nima.2011.01.092.
[23] T. Guo, Z. Liu, L. Cai, An improved force feedback control algorithm for active tendons, *Sensors* 12 (8) (2012) 11360–11371, http://dx.doi.org/10.3390/s120811360.
[24] J.P. Den Hartog, *Mechanical Vibrations*, 4th ed. Dover Publications, Inc., New York, 1985.
[25] P.B. Muanke, P. Masson, P. Micheau, Determination of normal force for optimal energy dissipation of harmonic disturbance in a semi-active device, *Journal of Sound and Vibration* 311 (3–5) (2008) 633–651, http://dx.doi.org/10.1016/j.jsv.2007.09.021.
[26] P.B. Muanke, P. Micheau, P. Masson, Nonlinear phase shift control of semi-active friction devices for optimal energy dissipation, *Journal of Sound and Vibration* 320 (1–2) (2009) 16–28, http://dx.doi.org/10.1016/j.jsv.2008.08.002.
[27] P. Dupont, A. Stokes, Semi-active control of friction dampers, *Proceedings of the 34th Conference on Decision & Control*, December, New Orleans, LA, 1995, pp. 3331–3336.
[28] J.L. Kuehn, H.L. Stalford, Stability of a Lyapunov controller for a semi-active structural control system with nonlinear actuator dynamics, *Journal of Mathematical Analysis and Applications* 251 (2) (2000) 940–957, http://dx.doi.org/10.1006/jmaa.2000.7177.
[29] L. Gaul, R. Nitsche, Friction control for vibration suppression, *Mechanical Systems and Signal Processing* 14 (2) (2000) 139–150, http://dx.doi.org/10.1006/mssp.1999.1285.
[30] M. Vidyasagar, *Nonlinear Systems Analysis*, 2nd ed. Prentice-Hall, Inc., Englewood Cliffs, NJ, 1993.
[31] J.-J.E. Slotine, W. Li, *Applied Nonlinear Control*, Prentice-Hall, Inc., Englewood Cliffs, NJ, 1991.